

## RAE

1. **TIPO DE DOCUMENTO:** Trabajo de grado para optar por el título de INGENIERO DE SONIDO.
2. **TITULO:** COMPARISON BETWEEN SOUND INSULATION PREDICTION MODELS FOR AIRBORNE NOISE TRANSMISSION.
3. **AUTOR:** Camilo E. De La Cruz F.
4. **LUGAR:** Bogotá D.C.
5. **FECHA:** Julio 2017.
6. **PALABRAS CLAVE:** Surface density, Single leaf wall, Critical Frequency, Ideal Sound Insulation Models, Double Leaf Wall.
7. **DESCRIPCION DEL TRABAJO:** El objetivo principal de este proyecto es analizar y comparar el comportamiento del aislamiento acústico alrededor del rango de la frecuencia crítica con diferentes modelos. Esto se hace con el fin de hallar un modelo que tenga una pequeña desviación con los diferentes software usados para predicciones de TL de distintos tipos de estructuras en Europa dando correcciones si necesarias al modelo establecido por Randall F. Barron. Se hace uso de la estadística descriptiva para hallar la desviación más pequeña y su correspondiente modelo. De esta manera, generando un estado de arte más actualizado para el uso de la universidad, facilitando la enseñanza de modelos actuales de aislamiento acústico a estudiantes en el futuro.
8. **LINEAS DE INVESTIGACION:** Línea de investigación de la USB: Acústica Aplicada. Programa: Ingeniería de Sonido
9. **METODOLOGIA:** Es de carácter empírico-analítico, enfocado en el análisis y comparación de diferentes modelos citados por software europeos.
10. **CONCLUSIONES:** De los software utilizados para comparar, se da una clara evidencia de que SoundFlow, de origen alemán, tiene una mejor capacidad de generar predicciones de aislamiento acústico para estructuras estilo particiones simples, dobles o multicapa (compuestos por 2 capas) cuando los valores de TL (Transmission Loss) son por encima de 80 [dB]. Esto se da porque dBKAisla, de origen español, tiene un limitante para sus predicciones de 80 [dB] sin importar la estructura que se utilice. Conclusiones de los modelos referenciados a distintos autores: *A diferencia del modelo presentado por Randall F. Barron que genera tres axiomas para el cálculo de la pérdida por transmisión (TL), David A. Bies presenta cinco axiomas que generan una curva en la región de la frecuencia crítica en vez de una conexión entre dos diferentes regiones de comportamiento de TL como se ve con Randall F. Barron. Debido a que el valor de Poissons's ratio es de cero a uno, su comportamiento puede ser eludido sin deteriorar las predicciones dadas por diferentes modelos presentado por varios autores, esto se puede evidenciar en la región de rigidez y masa. Además, Todos los modelos hacen uso de la frecuencia crítica para el mejoramiento de las predicciones de aislamiento acústico en la región de amortiguamiento.* Para los elementos multicapa (compuestos por dos capas) las estructuras delgadas tienen las menores desviaciones en las predicciones de aislamiento acústico cuando, se utiliza la definición de la frecuencia crítica de Randall F. Barron pero se usa el modelo de predicción de aislamiento acústico de David. A. Bies.

COMPARISON BETWEEN SOUND INSULATION PREDICTION MODELS FOR  
AIRBORNE NOISE TRANSMISSION

CAMILO E. DE LA CRUZ F.

UNIVERSIDAD DE SAN BUENAVENTURA  
FACULTAD DE INGENIERIA  
INGENIERIA DE SONIDO

BOGOTA D.C. - 2017

COMPARISON BETWEEN SOUND INSULATION PREDICTION MODELS FOR  
AIRBORNE NOISE TRANSMISSION

A thesis submitted in fulfillment of the requirements for the degree of Sound Engineering in  
Universidad de San Buenaventura by Camilo E. De La Cruz F.

Adviser: Felipe A. Vallejo Monsalve

Universidad de San Buenaventura, Bogotá D.C.

2017

## List of figures

|   |    |
|---|----|
| Figure 1 - Equal forces acting on a layer in opposite directions without change of volume.....  | 11 |
| Figure 2 - Visual representation of the simplest case in sound insulation studies.....  | 12 |
| Figure 3 - Sound Transmission from material 1 to material 3 .....   | 17 |
| Figure 4 – Objective 1 “Definition” .....   | 39 |
| Figure 5 – Objective 3 “Definition” .....   | 40 |
| Figure 6 – Mass Law Model Case 1 .....  | 44 |
| Figure 7 – David A. Bies 2 <sup>nd</sup> model, Reference to Davy .....   | 46 |
| Figure 8 – Low frequency event Case 13 .....  | 46 |
| Figure 9 – Transmission loss predictions from all models .....  | 48 |
| Figure 10 – Possible recommendation for transmission loss model .....   | 50 |
| Figure 11 – TL multilayer element Case 26 .....   | 51 |
| Figure 12 – Imaginary Bending Impedance vs Angle of Incidence (Res is 50 Hz, Blue is 63 Hz, Green is 80 Hz and it keeps increasing in one third octave bands) .....               | 52 |
| Figure 13 – Imaginary Bending Impedance vs Frequency (showing the frequency generated for different angles) .....   | 53 |
| Figure 14 – Extensional Impedance vs Angle of Incidence (for different frequencies beginning in 50 Hz and moving in one third octaves to 5kHz) .....                              | 54 |
| Figure 15 – Extensional Impedance vs Frequency (Blue is the Critical Frequency angles of incidence) ....  | 54 |
| Figure 16 – Bending Impedance vs Angle of incidence Bies-Cremer (Red is 50 Hz, Blue is 63 Hz, Green is 80 Hz and it keeps increasing in one third octave bands until 5 kHz) ..... | 55 |
| Figure 17 – Bending Impedance vs Frequency Bies-Cremer (Showing the frequency generated for different angles).....  | 56 |
| Figure 18 – Bending and compressional wave velocities (Red circles are Bies-Cremer and black stars are Sharp).....  | 57 |
| Figure 19 – dBKAisla ISO 12354 module .....   | 60 |
| Figure 20 – SPSS Analysis Cases 1-6.....  | 63 |
| Figure 21 – SPSS Analysis Cases 7-13.....   | 64 |
| Figure 22 – SPSS Analysis Cases 16-24.....  | 65 |
| Figure 23 – SPSS Analysis Cases 25.-27 .....  | 66 |

## List of tables

|  |    |
|--|----|
| Table 1 - State of the art Variables .....   | 7  |
| Table 2 - Reference information for the plateau area for the 1 <sup>st</sup> prediction method .....         | 19 |
| Table 3 - Averaging times/ Frequency Range .....   | 31 |
| Table 4 - Sound insulation reference values ISO 717-1 .....  | 32 |
| Table 5 - Adaptation Terms ISO 717-1 .....   | 32 |
| Table 6 – Solid Plate Properties .....   | 36 |
| Table 7 – Single Leaf, Double Leaf [ML: Model0 dBKAisla; CML:Model1 dBKAisla; BIS Model2 SoundFlow]<br>..... | 38 |
| Table 8 – Software Requirement Evaluation table .....  | 41 |
| Table 9 – Results sheet comparison .....   | 42 |
| Table 10 – Broadband quantity analysis Cases 1-6.....  | 43 |
| Table 11 – Prediction models variance Cases 1-6.....   | 43 |
| Table 12 – Broadband quantity analysis Cases 7-13.....   | 44 |
| Table 13 – Prediction models variance Cases 7-13.....  | 45 |
| Table 14 – Example of possible combinations for thickness h .....  | 47 |
| Table 15 – Broadband quantity analysis Cases 14-24.....  | 47 |
| Table 16 – Prediction models variance Cases 16-18.....   | 48 |
| Table 17 – Prediction models variance Cases 19-21.....   | 49 |
| Table 18 – Prediction models variance Cases 22-24.....   | 49 |
| Table 19 – Broadband quantity analysis Cases 25-27.....  | 50 |
| Table 20 – Prediction models variance Cases 25-27.....   | 51 |
| Table 21 – Cases 1-6 analysis .....  | 61 |
| Table 22 – Cases 7-13 analysis.....  | 61 |
| Table 23 – Cases 16-24 Analysis.....   | 61 |
| Table 24 – Cases 25-27 Analysis.....   | 62 |

|   |    |
|---|----|
| List of figures.....  | i  |
| List of tables.....   | ii |
| Introduction.....   | 1  |
| Chapter I .....   | 2  |
| 1.1    Problem Statement.....   | 2  |
| 1.1.1    Background.....  | 2  |
| 1.1.2    State of the Art.....  | 2  |
| 1.1.2.1    Airborne Sound Inuslation of wall structures – measurement and prediction methods.2000.....                | 2  |
| 1.1.2.2    Accuracy of Prediction Methods for Sound Transmission Loss. 2004.....                                      | 3  |
| 1.1.2.3    Comparison of the Models Predicting Sound Insulation of Multilayered Building Elements. 2012.....          | 4  |
| 1.1.2.4    The Sound Insulation of Cavity Walls. 2012.....  | 5  |
| 1.1.2.5    Recent advances in building acoustics: An overview of prediction methods and their applications. 2015..... | 6  |
| 1.1.2.6    Important attributes for different transmission loss analytical models.....                                | 7  |
| 1.2    Problem Description and Formulation.....   | 7  |
| 1.3    Justification.....   | 8  |
| 1.4    Research Objective.....  | 8  |
| 1.4.1    General Objective.....   | 8  |
| 1.4.2    Specific Objectives.....   | 9  |
| 1.5    Limitation and Delimitations.....  | 9  |
| 1.5.1    Limitations.....   | 9  |
| 1.5.2    Delimitation.....  | 9  |
| Chapter II.....   | 10 |
| 2.1    Theoretical Framework.....   | 10 |
| 2.1.1    Engineering Noise Control Theory and Practice.....   | 10 |
| 2.1.1.1    Transmission Loss theory.....  | 10 |
| 2.1.1.2    Panel Transmission Loss.....   | 12 |
| 2.1.1.3    Double Wall Transmission Loss.....   | 14 |
| 2.1.1.4    Multilayer structure.....  | 15 |
| 2.1.2    Industrial Noise Control and Acoustics.....  | 16 |
| 2.1.2.1    Transmission Loss theory.....  | 16 |
| 2.1.2.2    Approximate Method for Estimating the TL.....  | 18 |

|  |    |
|--|----|
| 2.1.2.3 A more intricate method that takes into account different variables as it builds the transmission loss curve. ....   | 19 |
| 2.1.2.4 Composite Wall with an Airspace Transmission Loss.....   | 21 |
| 2.1.3 Architectural Acoustics – Marshall Long .....  | 23 |
| 2.1.3.1 Transmission Loss Theory .....   | 23 |
| 2.1.3.2 Single Panel Transmission Loss .....   | 24 |
| 2.1.3.3 Double Leaf Transmission Loss.....   | 25 |
| 2.1.4 Accuracy of Prediction Methods for Sound Transmission Loss .....   | 26 |
| 2.1.4.1 Single Leaf Transmission Loss .....  | 26 |
| 2.1.4.2 Double Leaf Transmission Loss.....   | 26 |
| 2.1.5 The Transmission Loss of Multilayer Structures .....   | 27 |
| Chapter III.....   | 29 |
| 3.1 ISO 16283 “Field Measurement of Sound Insulation in buildings and of building elements” Part 1 Airborne sound insulation.....  | 29 |
| 3.2 ISO 717-1 “Rating of sound insulation in building and of building elements – Part 1 Airborne Sound Insulation”.....  | 32 |
| Chapter IV: Research Focus .....   | 34 |
| 4.1 Research Line.....   | 34 |
| 4.2 Data gathering techniques .....  | 34 |
| 4.2.1 User Manual Key information (SoundFlow) .....  | 34 |
| 4.2.2 User Manual Key information (dBKAisla).....  | 35 |
| 4.2.3 Common Ground .....  | 35 |
| Chapter V: Engineering Development.....  | 36 |
| 5.1 Methodology .....  | 36 |
| 5.1 .1Choosing software .....  | 36 |
| 5.1.2 Revising Literature.....   | 36 |
| 5.1.3 Construction of Sample size .....  | 37 |
| 5.1.4 Process to accomplish an analysis of the models used in sound insulation predictions tools like SoundFlow and dBKAisla for single, double and multilayer structures..... | 37 |
| 5.1.5 Steps to compare the prediction model used for multilayer components with Sharps method for multilayer elements.....   | 39 |
| 5.1.6 Process taken to evaluate the user interfaces for SoundFlow and dBKAisla.....  | 39 |
| Chapter VI: Results.....   | 41 |
| 6.1 Software Selection. ....   | 41 |
| 6.1.1 Software User Input and Result sheet .....   | 41 |

|  |    |
|--|----|
| 6.2 Single leaf, double leaf and multilayer structures.....        | 42 |
| 6.2.1 Mass Law Single Leaf .....                                   | 43 |
| 6.2.2 SoundFlow Single Leaf.....                                   | 44 |
| 6.2.3 SoundFlow Double Leaf .....                                  | 47 |
| 6.2.4 SoundFlow Multilayer Structure.....                          | 50 |
| 6.3 Multilayer Model .....   | 52 |
| 6.3.1 Implementation of a specific algorithm .....                 | 52 |
| 6.4 User Interface Evaluation .....                                | 57 |
| 6.4.1 dBKAisla.....  | 58 |
| 6.4.2 SoundFlow .....  | 59 |
| 6.4.3 Looking at some pros and cons.....                           | 59 |
| 6.5 Transmission loss and the weighted sound reduction index ..... | 60 |
| 6.6 ISO 717-1 .....  | 62 |
| Chapter VII: Discussion.....                                       | 67 |
| 7.1 Software Selection .....                                       | 67 |
| 7.2 Single Leaf, Double Leaf and Multilayer Structures .....       | 67 |
| 7.2.1 Mass Law Single Leaf .....                                   | 67 |
| 7.2.2 SoundFlow Single Leaf.....                                   | 67 |
| 7.2.3 SoundFlow Double Leaf .....                                  | 68 |
| 7.2.4 SoundFlow Multilayer Structure.....                          | 68 |
| 7.3 Multilayer Sharp .....   | 68 |
| 7.4 Transmission loss and the weighted sound reduction index ..... | 69 |
| 7.5 ISO 717-1 .....  | 69 |
| 7.6 Conclusions.....   | 70 |



*Abstract: This graduation project presents different theories for sound insulation models used in airborne transmission by the authors Randall F. Barron, David A Bies and Marshall Long and analyzes them against professional software used in Europe. The models present good agreement in the frequency range above the critical frequency. The models are analyzed using descriptive statistics on the predictions for transmission loss in architectural structures like single leaf, double leaf and multilayer elements composed of two layers. From the transmission loss predictions, the range below the critical frequency presents the largest discrepancy to the software used as references which are SoundFlow and dBKAisla. The multilayer model presented by B.H.S Sharp is compared to the multilayer model presented by David A. Bies to identify some differences and similarities and the bending impedance and compressional wave velocity are identified as variables that showcase this notion. The software that was chosen as a reference depends on the type of structure that is being used. For thin panels that have transmission loss values that are below 80 [dB] the reference is chosen as dBKAisla and for structures that have transmission loss values above 80 [dB] the reference is chosen as SoundFlow.*



## **Introduction**

The implementation of lightweight building materials is a leading cause to extensive research into the sound transmission loss of specific types of wall systems in different regions of the world (Cambridge, 2012). Because of this, the need to obtain a more comprehensive understanding of different available prediction models or methods used to calculate sound insulation for airborne noise transmission, can help with the transition of heavyweight building materials to lightweight building materials as well as reducing the costs of a building construction in some occasions without having to compromise sound insulation. The ability of differentiating the common grounds used for sound insulation between different authors can help further the knowledge and understanding of transmission loss models used for predicting the behavior of different types of walls and structures in order to obtain a required or desired sound insulation value. For this purpose, two software are chosen as reference models to analyze and investigate. Looking at the different models, the results will be analyzed and compared to a chosen reference depending on the type of element that is used. The critical frequency is one of the defining attributes used to create a transmission loss curve for a construction element whether it is a single leaf, double leaf or multilayer element (these are the type of elements presented in this thesis). Considering this, and the different models that are presented by various authors, this thesis work aims to bring an amalgamation to generate better predictions when looking at software used in Europe. The authors of interest considered to present a recommendation to the models used in transmission loss are: Randall F. Barron, David A. Bies, Marshall Long and B.H.S Sharp. These theories are applied in Australia, U.S.A, and England, among other countries. The purpose of these predictions is to show a general idea of the behavior in a construction element when dealing with sound insulation.

## Chapter I

### 1.1 Problem Statement

There are no studies that depict how theories presented in architectural acoustics differ in sound insulation predictions for airborne noise transmission, when looking at studies in a local area. This opens the opportunity of using a MATLAB classroom license for instructional use to assist in a learning environment when studying transmission loss. This will be accomplished using a function which showcases the principle considerations for sound insulation models, its solid plate properties and its dependent variables for each type of structure. The sound insulation models for airborne noise transmission will be analyzed using descriptive statistics (Kurra, 2012). The goal of using descriptive statistics is to find the variation that is presented by the different theoretical models. And the analysis for this project is, to compare the calculated results and investigate a better pairing if possible.

#### 1.1.1 Background

The model presented by Randall F. Barron (Barron, 2003) can be analyzed with other models to see how it behaves when compared with some of the software available in Europe. In Germany, there is a software used to generate sound insulation predictions for structures such as single leaf, double leaf and multilayer. AFMG SoundFlow. In Spain, there is another software used for the same purpose. dBKAisla. These two software use models that differ when predicting transmission loss values and give a range of where transmission loss values should be when looking at different types of structures.

#### 1.1.2 State of the Art

##### 1.1.2.1 Airborne Sound Insulation of wall structures – measurement and prediction methods.2000

This is a thesis document that was presented at the Helsinki University of Technology in Finland for the degree of Doctor in Science. The purpose of the thesis was to study and compare the validity of different physical models used to predict sound insulation of wall structures, as well as, to study the benefits of using the sound intensity measurement method vs the pressure method for determining sound insulation. Valtteri Hongisto dedicates a section of the document to give a general overview of the prediction models and a brief introduction to different types of single walls.

These single walls or single panels, are divided into four main types of panels. The types of panels given by Hongisto are: thin panels, corrugated panels, stiffened panels and thick monolithic panels. For thin panels the main factors defined, that determine the transmission loss of the structure are the surface mass, bending stiffness, dimensions, loss factor and sound incidence angle. The monolithic thick walls behave differently than thin panels and a wall is defined as acoustically thick when  $1/3$  to  $1/6$  of the bending wavelength of the panel is less than the thickness of the panel. The

materials used in construction can also lead to a thick panel type of construction. For example, Hongisto mentions that the materials which are classified as thick panels are brick, heavy concrete and porous concrete. The reason is that such materials tend to have a large bending stiffness, displacing the critical frequency to low frequencies that tend to be below 200 [Hz]. This occurs because, for thick panels, the shear waves become the dominant force which shape the sound transmission. To this, Hongisto cites Rindel to having proposed an effective bending stiffness,  $B_{eff}$ , that considers the effect of the shear waves. Continuing with the definition of different types of structures, Hongisto also defines double walls as ideal or uncoupled when using prediction models that do not consider inter-panel connections when predicting sound transmission. In the conclusions, Hongisto states that for double panels, some models give variations that exceed 20 [dB] and sometimes even reach values as high as 40 [dB].

#### **1.1.2.2 Accuracy of Prediction Methods for Sound Transmission Loss. 2004**

This is an article that was presented in the 33<sup>rd</sup> international congress and exposition of noise control engineering. Ballagh presents some evidence that for an engineer to give a solution to specific problems found in architectural acoustics when dealing with noise levels or acoustic privacy between adjacent rooms or apartments, it is important to know the sound transmission loss for the construction structures that will be used in a building and thus it is a pressing matter to have reliable methods for predicting the general behavior of different types of structures used in architectural acoustics. In his article, author K.O. Ballagh, compares experimental measurements of transmission loss and theoretical models used for sound insulation predictions. Two types of structures are analyzed by Ballagh. The first is the single leaf homogenous panel and the second is the double leaf partition. Between both structures the variables are mass, stiffness, damping, panel size, air gap between panels, connections between panels and acoustic absorption in the cavity. For the simplest transmission loss prediction, the mass law is often used because it accounts for the surface density also known as the mass per unit area of the panel (this is intended for single leaf homogenous non-porous panels). This in turn gives a simple model that is easily and readily available for thin homogenous materials, the mass law can be modified to account and include the variations in transmission loss given at the critical frequency and above, when coincidence between airborne and structure borne waves occurs. Ballagh states that, when using concrete or brick as the building materials, the expressions given in the paper are not reliable because the transmission loss is affected by the shear waves reducing the transmission loss of the elements. Ballagh, defines the simplest case in double panels as two thin homogenous panels separated by an air gap containing acoustically absorbent material with no interconnections between the panels. Because many walls and floors are built in such a manner, it is usually a necessity to calculate the transmission loss of such elements. A model for double leaf wall transmission loss predictions, working in three different frequency ranges, is presented and referenced to Sharp but it does not consider the effect of the acoustic absorbent material inside the cavity of the double leaf partition.

To correct this failure, an alternative that considers the acoustic absorbers in the airspace is presented by Fahy for the high frequency range. In the conclusions, Ballagh, states that the prediction methods are fairly reliable and acceptable. Does so because the measurement repeatability and reproducibility should not go beyond  $\pm 2$ [dB] and should be considered when working with masonry or lightweight building constructions in the frequency range of 50-5k [Hz].

### **1.1.2.3 Comparison of the Models Predicting Sound Insulation of Multilayered Building Elements. 2012**

This is an article presented in the Elsevier journal from Turkey. Selma Kurra states that several models for transmission loss predictions have been developed by various authors. Uses descriptive statistics to analyze and observe  $R_w(C, C_{tr})$  and indicate which models have a higher correlation when compared to each other. The largest difference between all models is found in the high frequency range using 1/3 octave band analysis. Moving on, from an acoustical vantage point, Kurra defines different types of constructions used in architectural acoustics. Some of these are, the single leaf wall, the double leaf wall and a multilayer element. With the different types of structures in mind, it can be inferred that the transmission loss is dependent on specific parameters in each type of structure. This resulting in different sound insulation values for the same type of element when using different theoretical models. This can be used to show the importance of being able to determine transmission loss using a model that when employed is reliable. To choose different software and models, Selma Kurra considers the following 6 points. 1. Uses the basic theories that are well documented. 2. Airborne sound insulation can be calculated for single leaf, double leaf and multilayer elements with these models. 3. The models take into account the dimensions of the type of structure. 4. The software functions as an independent application in the Windows OS. 5. The software gives a report of a global index or single number rating for the sound insulation as well as tables and diagrams. 6. The software has its own material database but also allows the user to input a new material with its physical properties like density, elasticity modulus, poisson's ratio, loss factor and size of element. The objectives of the statistical analysis employed by Kurra were: The verification of the calculated results with experimental data and the investigation of the differences between the models and their best matching, the comparison of the calculated results from each individual model. To investigate the differences between the models transmission loss and the single number rating, Kurra presents a table that superposes the  $R_w(C)$  values. This is presented with different curves in a graph, where the x-axis is the case number and the y-axis are the different single number ratings obtained from the different models. Looking at which models have the smallest mean variation as well as standard deviation, Kurra obtains evidence that two models are closer in the mean while in the standard deviation they are further apart than the variation of the other model. In the results, the weighted sound reduction index is altered from each model because the software using different models calculate R values in different frequency ranges.

Where the first uses the 50 [Hz] to 5 [kHz], the second uses the 60 [Hz] to 6.3 [kHz] and the third uses the 100 [Hz] to 5 [kHz]. This in terms affects not only the weighted sound reduction index with the spectral adaptation terms but also the statistical analysis when comparing the different models.

#### **1.1.2.4 The Sound Insulation of Cavity Walls. 2012**

This is a thesis document submitted for the degree of doctor of philosophy at the university of Canterbury in New Zealand by Jason Cambridge. In this thesis, the following is presented.

Lightweight materials are being used in building constructions and because of this, the sound transmission loss of double leaf wall systems is being researched. To this end, there is a need to obtain a comprehensive understanding of the influence of the absorption material in the cavity of the double leaf wall system. Cambridge mentions that, existing prediction models do not agree with some observed experimental results and thus gives evidence for the need of studying the influence of the absorption material. More evidence for the study is given because different countries have developed building codes that stipulate requirements for sound transmission loss and although the requirements vary according to the country, it is globally accepted that the health and wellbeing of the people or population is affected by noise. Cambridge also gives an example of a typical double leaf wall system used to separate two rooms, as seen in the simplest case in sound insulation. For the double leaf wall system, there are specific frequencies that are taken into account when the transmission loss is calculated. The first frequency presented for this is, the mass air mass resonance frequency which marks the dominance of the mass of the panel below said frequency. The second frequency presented is the limiting frequency and Cambridge states that for frequencies greater than said frequency, the wavelength of the sound wave within the cavity becomes comparable to and less than the panel separation. Within the second frequency range, the behavior presented by the cavity resonance perpendicular to the wall plays the main role in determining the transmission loss. The third frequency given for double leaf wall systems, is the critical frequency which also has a great value when predicting transmission loss for single leaf panels. Cambridge justifies the research for two reasons. One. Existing prediction models are not able to explain observed experimental trends. Two. The interaction between the forced and reflected forced waves along the cavity is a crucial component to obtain a more comprehensive understanding of the sound transmission below the critical frequency for the double leaf wall system. And adding more fuel to the fire, Cambridge also states that Hongisto did a survey in 2006 which presented a high degree of variability in the results of an entire spread of commercially available walls.

### **1.1.2.5 Recent advances in building acoustics: An overview of prediction methods and their applications. 2015**

This is an article presented in the Elsevier journal from Hong Kong.

Mak presents an overview of different prediction methods used in building acoustics and states that the analytical models have made headway in the contributions to the research literature in architectural acoustics. Also, focuses mainly in predictions of sound in room acoustics and limits the behavior to airborne sound. In order to properly evaluate an acoustical environment, Mak states that one must have the essential and appropriate methods for predicting the level and spectral content that will be inside the building or construction. For this purpose, this article reviews some of the studies related to the prediction methods used in building acoustics in English-language journals to present a clear overview of the recent advances in building acoustics, and the methods used for predicting sound fields in buildings, noting that there are methods for room acoustics, airborne sound transmission, structure borne transmission and duct borne transmission among others.

In the overview of the prediction methods for airborne sound, the definition of airborne sound is given as sound that is generated in a room and can be transferred to adjacent rooms via different transmission paths such as walls, floors, building framework and interconnecting ducts. It also defines “airborne sound insulation” as the net reduction of airborne sound energy caused by the sound transmission between rooms via one of the available and aforementioned paths. Also, the simplest case is introduced as rooms being separated by a homogenous, non-porous single leaf wall when the use of the mass law has been inherently connected to the prediction of its transmission loss. To this, it is considered that the elements most worked on, when thinking of the simplest case in architectural acoustics for transmission loss, are the single leaf and double leaf wall as well as multilayer elements. A definition of the mass law is given and it is clear that the surface density and the characteristic air impedance is used to calculate the transmission loss at a given frequency.

In the overview, Mak notes that several authors have worked on different models to predict transmission loss for various types of structures. Some of these authors are Hongisto V in “Sound insulation of double panels-comparison of existing prediction models”, Kurra S in “Comparison of the models predicting sound insulation values for multilayered building elements”, Nakanishi S, Yairi M and Minemura A in “Estimation method for parameters of construction on predicting transmission loss of double leaf dry partition”, among others that may have been published in non-English language journals. This serves to show that studies dealing with transmission loss are still being published and reviewed globally.

To conclude, Mak mentions that there are many aspects in building acoustics and that the article has only focused in reviewing recent research to provide an indication of the advances in prediction methods presented in architectural acoustics. Mak also



notes that, in the past three years the major contributions to the field of architectural acoustics prediction methods came from analytical models related to the prediction of sound in a room and for airborne sound transmission.

### 1.1.2.6 Important attributes for different transmission loss analytical models

In Table 1 we see the recurrent variables that are presented in different works of literature covered in the state of art. In the # column, the number represents the article in the state of the art. They are in the same order as presented above.

Table 1 - State of the art Variables

| E | $\eta$ | $\sigma$ | B | $h$ | $\rho_m$ | $M_s$ | $Z_{air}$ | $f_c$ | $f_{in}$ | $a$ | $b$ | $d$ | $\alpha$ | # |
|---|--------|----------|---|-----|----------|-------|-----------|-------|----------|-----|-----|-----|----------|---|
|   | ■      |          | ■ | ■   |          | ■     |           | ■     | ■        | ■   | ■   |     |          | 1 |
|   | ■      |          | ■ |     |          | ■     |           | ■     |          | ■   | ■   | ■   | ■        | 2 |
| ■ |        | ■        |   | ■   | ■        |       |           |       |          | ■   | ■   |     |          | 3 |
|   |        |          |   |     |          |       |           | ■     | ■        |     |     |     |          | 4 |
|   |        |          |   |     |          | ■     | ■         |       |          |     |     |     |          | 5 |

## 1.2 Problem Description and Formulation

Considering that various authors have developed their own empirical formulas and some have even done comparisons between prediction methods for sound insulation, as shown above, sound insulation prediction is a subject that continues to grow and is still studied to better predict values for different types of elements (Mak & Wang, 2015). The available software for sound insulation predictions that deal with single leaf, double leaf and multilayer elements have a range of difference in the values that are given in the result sheet. This happens because they use different analytical models to predict the transmission loss of any type of structure. Also, thanks to authors who have compared different prediction models used in available software, that is either free or has a varying cost, descriptive statistics (Kurra, 2012) can be used to better assess and analyze how much each model differs from each other (and to this, the implementation of ISO 717-1). Because of this, there can be a tendency to ask how much do the values of sound insulation predictions from different models vary for airborne noise transmission. Also, it can lead to ask which models give reliable results when predicting the general behavior for different types of structures.

## **1.3 Justification**

The purpose of a sound insulation prediction software is to give a general idea of how a construction element will behave when finished, considering its acoustic properties/characteristics. This in hand, goes with a broader understanding of the different sound insulation prediction models that are being used by different software allowing to showcase some unique features of each other.

As a summary concluding from the information presented in the state of the art and problem statement. We get the following:

1. Considering the first reference in the state of the art where some models give variations that exceed 20 [dB] in double leaf panels, it starts to become clearer that a study to analyze different models should be looked into. From this, the theoretical models will present different results in the thesis project because of the aforementioned evidence from the first reference.
2. In the second reference of the state of the art, the author presented notes that there is a pressing matter to have reliable methods for predicting the general behavior of different types of structures used in architectural acoustics. This leads to ponder about which theoretical models are reliable methods to predict the general behavior of different types of structures and what type of structure.
3. In the third reference, the author states that the highest variation seen in the transmission loss between the studied models is found in the high frequency range when analyzing the results in 1/3 octave bands. Also, something that can be seen when using different theoretical models to predict the transmission loss is that, the same element can give different results in the sound insulation. Showing the importance of finding a reliable model to use when predicting the sound insulation values of a type of structure. Because of this third reference, the hypothesis is to expect larger deviations in the transmission loss values in the high frequency range.

## **1.4 Research Objective**

### **1.4.1 General Objective**

To analyze and compare the behavior around the critical frequency range with different models used for airborne sound insulation predictions.

## **1.4.2 Specific Objectives**

-To analyze the models used in sound insulation prediction tools like soundflow and dBKAisla for single, double and multilayer structures.

-To compare the prediction model used for multilayer components with Sharps methods for multilayer elements.

-To evaluate the user interfaces for SoundFlow and dBKAisla.

## **1.5 Limitation and Delimitations**

### **1.5.1 Limitations**

This thesis work will explore models that predict transmission loss for single leaf structures, double leaf structures and multilayer elements considering the range of difference in the predictions from different software available in Europe.

### **1.5.2 Delimitation**

Thirty cases will be presented to analyze and compare transmission loss models used for sound insulation predictions for airborne transmission. The software chosen to evaluate is SoundFlow and dBKAisla, the latter is from Spain and the former from Germany. Functions will be developed for MATLAB as an instructional tool for the different models used.

## Chapter II

### 2.1 Theoretical Framework

#### 2.1.1 Engineering Noise Control Theory and Practice

The following is a brief summary of chapter 8 Partitions, Enclosures and Barriers covering introduction, panel transmission loss and double panel transmission loss(A. Bies & H. Hansen, 2003).

##### 2.1.1.1 Transmission Loss theory

The possibility of interrupting the transmission path from a source to a receiver/listener by placing a type of barrier between them is a form of airborne noise control. This gives a priority to the properties of the materials and structures to present and even consider the concept of transmission loss(A. Bies & H. Hansen, 2003). The interruption of the transmission path between source and receiver/listener considers three types of wave propagation inside a solid material to help control the airborne sound transmission. The critical frequency,  $f_c$ , defines the frequency for which airborne and solid borne wave speeds are equal as mentioned by the author David A. Bies (A. Bies & H. Hansen, 2003), the surface density of the panel,  $M_s$ , and the bending stiffness,  $B$ , are also defined as:

$$M_s = \rho_w h \quad [Eq \ 1]$$

Where  $\rho_w$  represents the density of the material and  $h$  represents the thickness of the barrier.

$$B = Eh^3/12(1 - \sigma^2) \quad [Eq \ 2]$$

Where  $E$  stands for Young's modulus and  $\sigma$  stands for Poisson's ratio.

$$f_c = \frac{c_{air}^2}{2\pi} \sqrt{\frac{M_s}{B}} \quad [Eq \ 3]$$

Where  $c_{air}$  stands for the speed of sound in air.

The critical frequency, which the author David A. Bies (A. Bies & H. Hansen, 2003) mentions is sometimes called the coincidence frequency, it exists for any panel that is capable of sustaining shear stress. Shear is the change of shape of a layer in a substance produced by a pair of equal acting forces in opposite directions along the two faces of the layer while there is no change of volume. (Figure 1) This figure was constructed with Sketch up to show the direction of the two acting forces.

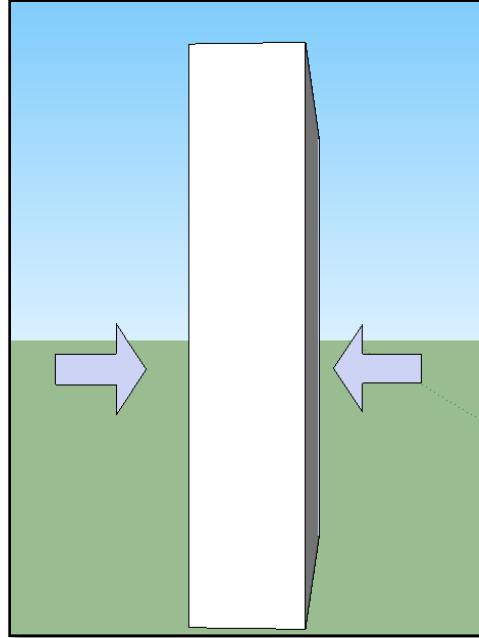


Figure 1 - Equal forces acting on a layer in opposite directions without change of volume

Another frequency used to determine the transmission loss is the lowest order frequency, commonly known as the fundamental frequency of a panel,  $f_{i,n}$ , and is given by:

$$f_{i,n} = \frac{\pi}{2} \sqrt{\frac{B}{M_S} \left[ \frac{i^2}{a^2} + \frac{n^2}{b^2} \right]} \text{ Hz} \quad [\text{Eq 4}]$$

Where  $i = n = 1$  when solving for the lowest order frequency.

The transmission coefficient  $\tau$  is the fraction of incident energy that is being transmitted from the source room to the receiver room through a partition or wall.

$$TL = -10 \log_{10}(\tau) \text{ dB} \quad [\text{Eq 5}]$$

The transmission loss is also dependent on the angle of incidence of the source and the power that is transmitted through the wall. The power transmitted through the wall  $w_t$  can be determined with the sound pressure in the source room  $\langle p_i \rangle$ , the surface area of the common partition between both rooms  $A$  and the air impedance  $Z_{air}$  with:

$$w_t = \frac{\langle p_i^2 \rangle A \tau}{4Z_{air}} \quad [\text{Eq 6}]$$

The air impedance can be defined using the density of the air and the speed of sound in air:

$$Z_{air} = \rho_{air} c_{air} \quad [\text{Eq 7}]$$

By using the sound pressure in the receiving room,  $S$  can be defined as the absorption area of the receiving room and  $\bar{\alpha}$  as the mean Sabine absorption coefficient.

$$\langle p_r^2 \rangle = \frac{\langle p_i^2 \rangle A \tau (1 - \bar{\alpha})}{S \bar{\alpha}} = \frac{4w_t Z_{air} (1 - \bar{\alpha})}{S \bar{\alpha}} \quad [\text{Eq 8}]$$

Allowing to find the noise reduction or transmission loss with:

$$NR = 10 \log_{10} \frac{\langle p_r^2 \rangle}{\langle p_s^2 \rangle} = TL - 10 \log_{10} \frac{A(1-\bar{\alpha})}{s\bar{\alpha}} \quad [Eq 9]$$

This is pertinent when working in a diffuse field, seen in field measurements in the simplest case in sound insulation studies as shown in figure 2:

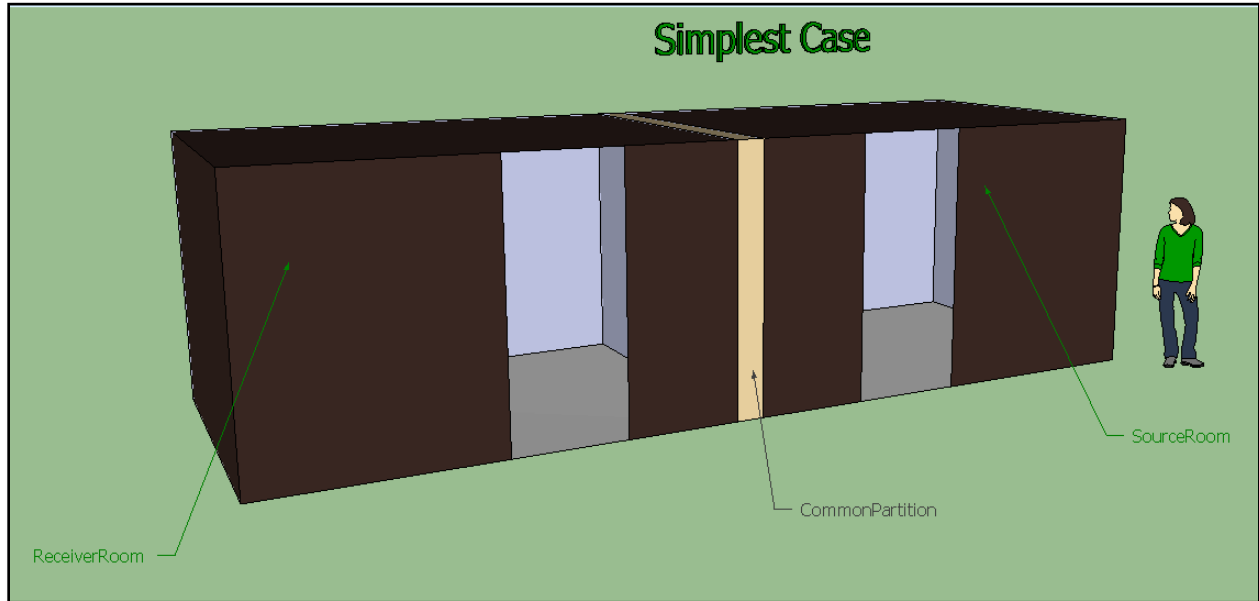


Figure 2 - Visual representation of the simplest case in sound insulation studies.

Again, Figure 2 is created using sketch up to give a visual aid of the simplest case in sound insulation. Where the receiver and source room are separated by a common partition.

### 2.1.1.2 Panel Transmission Loss

For panel transmission loss (thin panel), author David A. Bies (A. Bies & H. Hansen, 2003) presents two prediction models for the transmission loss where a curve is constructed based on two dominant curves. The first dominant curve is given by:

$$TL = 20 \log_{10} \left( \frac{\pi f M_s}{Z_{air}} \right) - 5.5 \text{ dB} \quad [Eq 10]$$

Equation [10] is commonly known as the mass law and presents one of its known variations. This curve only considers the surface density of the panel  $M_s$ .

The second dominant curve, that is used to construct the transmission loss prediction in both prediction models, takes into account the loss factor  $\eta$  as presented in the following equation as well as the critical frequency  $f_c$ :

$$TL = 20 \log_{10} \left( \frac{\pi f M_s}{Z_{air}} \right) + 10 \log_{10} \left( \frac{2\eta f}{\pi f_c} \right) \text{ dB} \quad [Eq 11]$$

For the first prediction scheme given by David A. Bies in Engineering Noise Control Theory and Practice(A. Bies & H. Hansen, 2003), cited to Sharp B.H., the following is presented:

- When  $f < \frac{f_c}{2}$  equation [10] is used to determine the transmission loss.
- When  $f \geq f_c$  equation [11] is used to determine the transmission loss.

Two points are used to intersect these two curves in the prediction scheme and are defined as:

$$PointA = 20 \log_{10}(f_c M_s) - 54 \text{ dB} \quad [Eq 12]$$

Where point A is located on  $\frac{f_c}{2}$ .

$$PointB = 20 \log_{10}(f_c M_s) + 10 \log_{10}(\eta) - 45 \text{ dB} \quad [Eq 13]$$

Where point B is located on  $f_c$ .

For the second prediction scheme found in Engineering Noise Control Theory and Practice by David A. Bies(A. Bies & H. Hansen, 2003), cited to Davy J.L., the following is presented:

- When  $f_0 < f < \frac{f_c}{2}$  equation [10] is used to determine the transmission loss.
- When  $\frac{f_c}{2} \leq f < 0.95f_c$  the following equations determine the transmission loss:

$$\theta_L = \cos^{-1} \left( \sqrt{\frac{\lambda}{2\pi\sqrt{A}}} \right) \quad [Eq 14]$$

Here  $\theta_L$  is a limiting angle presented by theories referenced to Davy J.L.

$$a(f) = \left( \frac{\pi f M_s}{\rho_0 c_0} \right) \left[ 1 - \left( \frac{f}{f_c} \right)^2 \right] \quad [Eq 15]$$

Here  $a$  is a function of frequency.

$$TL = 20 \log_{10} \left( \frac{\pi f M_s}{Z_{air}} \right) + 20 \log_{10} \left[ 1 - \left( \frac{f}{f_c} \right)^2 \right] - 10 \log_{10} \left[ \log_e \left( \frac{1+a^2}{1+a^2 \sin^2 \theta_L} \right) \right] \text{ dB} \quad [Eq 16]$$

When  $f \geq 1.2f_c$  the transmission loss is determined by:

$$TL = 20 \log_{10} \left( \frac{\pi f M_s}{Z_{air}} \right) + 10 \log_{10} \left[ \left( \frac{2\eta}{\pi} \right) \left( \frac{f}{f_c} - 1 \right) \right] \text{ dB} \quad [Eq 17]$$

When  $0.95f_c < f < 1.2f_c$  the transmission loss is given by:

$$\Delta_b = 0.236 \quad [Eq\ 18]$$

Used for 1/3 octave bands.

$$\Delta_b = 0.707 \quad [Eq\ 19]$$

Used for octave bands.

The  $\Delta_b$  is a ratio of the filter bandwidth to the filter center frequency as mentioned by David. A. Bies.

$$TL = 20 \log_{10} \left( \frac{\pi f M_s}{\rho_0 c_0} \right) + 10 \log_{10} \left[ \frac{2\eta \Delta_b}{\pi} \right] \quad dB \quad [Eq\ 20]$$

### 2.1.1.3 Double Wall Transmission Loss

The double wall construction introduces three important frequencies that are used to determine the transmission loss. The first frequency presented is the lowest order acoustic resonance  $f_2$ :

$$f_2 = \frac{c}{2L} \text{ Hz} \quad [Eq\ 21]$$

Where  $L$  is taken as the longest dimension of the cavity.

Another important frequency that is presented, is the lowest order structural resonance which is understood to represent the lowest order cavity resonance.

The author David A. Bies adds an empirical factor to give better agreement with existing data for ordinary wall constructions (A. Bies & H. Hansen, 2003). This empirical factor is used to make up for the effective mass of the panels being less than its actual mass since it is assumed that the two panels are limp masses connected by a massless compliance. The lowest order cavity frequency  $f_0$  is given by:

$$f_0 = \frac{1}{2\pi} \left( \frac{1.8 \rho_{air} c_{air}^2 (M_{s1} + M_{s2})}{d M_{s1} M_{s2}} \right)^{1/2} \text{ Hz} \quad [Eq\ 22]$$

Where  $M_{s1}$  stands for the surface density of the first panel and  $M_{s2}$  stands for the surface density of the second panel.

The final frequency that is used to determine the transmission loss is the limiting frequency,  $f_l$ , and it is used to determine a relation between the air gap and the panels in the double leaf structure.

$$f_l = \frac{c}{2\pi d} = \frac{55}{d} \text{ Hz} \quad [Eq\ 23]$$

Using these frequencies, various equations are used to establish and determine the transmission loss for the double wall type of structure. Note: The inside of the cavity is usually assumed to have a specific/random amount of absorption material inserted so that there are no standing waves in the air gap.



For the prediction scheme presented by David A. Bies(A. Bies & H. Hansen, 2003) for double leaf structures, we get the following. The first range is established when any frequency is below the lowest order cavity frequency, in other words:

$$f \leq f_0$$

Making  $M$  the total surface density of the double leaf wall structure:

$$M = M_{s1} + M_{s2} \quad [Eq \ 24]$$

The variables  $M_{s1}$  and  $M_{s2}$ , again, are the surface densities of each panel composing the double leaf panel. The mass law transmission loss of the double leaf panel is given by:

$$TL_M = 20 \log_{10} \left( \frac{\pi f M}{Z_{air}} \right) - 5.5 \text{ dB} \quad [Eq \ 25]$$

The second range is determined by any frequency being above the lower order cavity frequency and being below the limiting frequency, in other words:

$$f_0 < f < f_l$$

Where the transmission loss in this region is composed of:

$$TL = TL_1 + TL_2 + 20 \log_{10}(fd) - 29 \text{ dB} \quad [Eq \ 26]$$

Making the transmission loss of the first panel,  $TL_1$ :

$$TL_1 = 20 \log_{10} \left( \frac{\pi f M_{s1}}{Z_{air}} \right) \text{ dB} \quad [Eq \ 27]$$

And the transmission loss for the second panel,  $TL_2$ :

$$TL_2 = 20 \log_{10} \left( \frac{\pi f M_{s2}}{Z_{air}} \right) \text{ dB} \quad [Eq \ 28]$$

The third and final range is given when any given frequency is above or equal to the limiting frequency, in other words:

$$f \geq f_l$$

$$TL = TL_1 + TL_2 + 6 \text{ dB} \quad [Eq \ 29]$$

#### 2.1.1.4 Multilayer structure

For a multilayer structure composed of two laminates the author gives the following definition for the bending stiffness:

$$B_{eff} = \frac{E_1 h_1}{12(1-\sigma^2)} \left[ h_1^2 + 12 \left( y - \frac{h_1}{2} \right)^2 \right] + \frac{E_2 h_2}{12(1-\sigma^2)} \left[ h_2^2 + 12 \left( y - (2h_1 + h_2)/2 \right)^2 \right] \quad [Eq \ 30]$$

$$y = \frac{E_1 h_1 + E_2 (2h_1 + h_2)}{2(E_1 + E_2)} \quad [Eq \ 31]$$

$$M = \rho_1 h_1 + \rho_2 h_2 \quad [Eq \ 32]$$

$$f_c = \frac{c_{air}^2}{2\pi} \sqrt{\frac{M}{B_{eff}}} \quad [Eq \ 33]$$

## 2.1.2 Industrial Noise Control and Acoustics

The following is a brief summary of Chapter 4: Transmission of Sound (Barron, 2003).

### 2.1.2.1 Transmission Loss theory

The definition of the sound power transmission coefficient is given as, the ratio of the transmitted acoustic power to the incident acoustic power with the use of the characteristic impedances of each medium.

$$\alpha_t = \frac{4Z_1 Z_2}{(Z_1 + Z_2)^2} \quad [Eq \ 34]$$

Where  $Z_1$  stands for the impedance of the first medium and  $Z_2$  for the second medium. The above equation gives the sound power transmission coefficient for a sound wave moving from a medium 1 to a medium 2. With it, the transmission loss can be obtained using:

$$TL = 10 \log_{10} \left( \frac{1}{\alpha_t} \right) \text{ dB} \quad [Eq \ 35]$$

To look at sound transmission through a wall, first we consider that a sound wave strikes the interface of the wall at normal incidence. The acoustic pressure and particle velocity in each medium is expressed as a different function of  $p_{media}(x, t)$  and  $u_{media}(x, t)$  giving the following 2 relations, considering its boundary conditions on both sides of the wall:

$$p_1(0, t) = p_2(0, t) \text{ and } u_1(0, t) = u_2(0, t) \quad [Eq \ 36]$$

$$p_2(h, t) = p_3(h, t) \text{ and } u_2(h, t) = u_3(h, t) \quad [Eq \ 37]$$

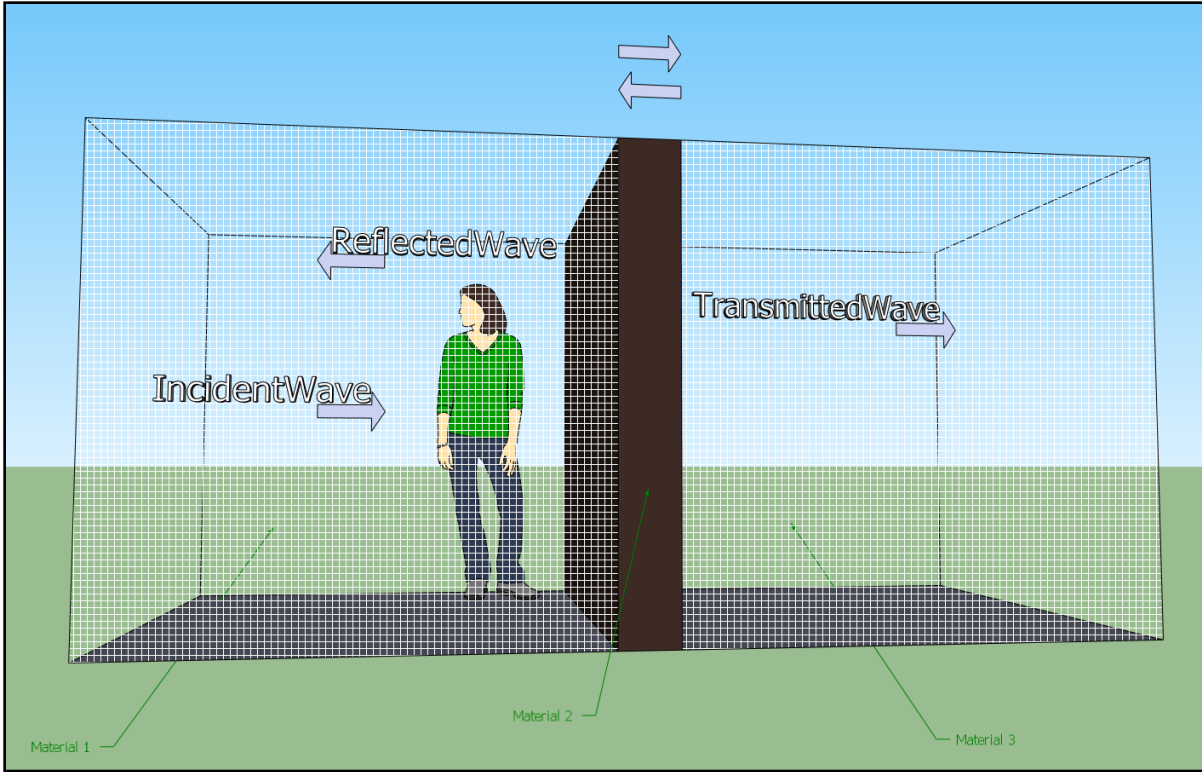


Figure 3 - Sound Transmission from material 1 to material 3

Giving a sound power transmission coefficient,  $a_t$ , from media 1 through media 2 to media 3 as:

$$a_t = \frac{4(Z_1/Z_3)}{\left(1 + \frac{Z_1}{Z_3}\right)^2 \cos^2(k_2 h) + \left(\frac{Z_1 + Z_2}{Z_2 + Z_3}\right)^2 \sin^2(k_2 h)} \quad [Eq\ 38]$$

Where  $k_2 h$  is expressed in radians as mentioned by the author Randall F. Barron and  $h$  stands for the thickness of the wall.  $Z_3$  stands for the impedance of the third medium.

For this sound power transmission coefficient, a case will be presented defining the sound power transmission coefficient:

This case is given when  $Z_1 = Z_3$

Meaning that the impedance,  $Z_1$ , in material 1 or media 1 is equal to the impedance,  $Z_3$ , in material 3 or media 3. This case also considers the following conditions:

1.  $Z_1 \ll Z_2$
2.  $(k_2 h) \leq 0.25$  [radians]
3.  $k_2 = \frac{2\pi f}{c_2}$  This is a simple rewriting of  $k_2$
4.  $M_s = \rho_2 h$  This is the specific mass

Giving the final sound power transmission coefficient as:

$$\frac{1}{a_t} = 1 + \left( \frac{\pi M_s f}{Z_{air}} \right)^2 \quad [Eq 39]$$

This case is most commonly known as the mass law.

The transmission loss is determined by:

$$TL = 10 \log_{10} \left( \frac{1}{a_t} \right) \text{ dB} \quad [Eq 40]$$

To calculate a transmission loss curve, the author Randall F. Barron offers two methods. The first is the Approximate method for estimating the transmission loss and the second is a more intricate method that takes into account different variables as it builds the transmission loss curve.

### 2.1.2.2 Approximate Method for Estimating the TL.

Regions II and III – are calculated based on an approximate method referenced by the author Randall F. Barron to another author.

One given assumption is that the panel dimensions need to be at least 20 times greater than the panel thickness so that the first resonance frequency can be under 125 [Hz]. The author also, mentions to the reader that one should always check the importance of the behavior of region I for the partition or element that will be analyzed. With this in mind, there is no equation given for the 1<sup>st</sup> region of transmission loss in single homogenous panels.

Region I

Region II

$$TL = TL_n - 5 = 10 \log_{10} \left[ 1 + \left( \frac{\pi M_s f}{Z_{air}} \right)^2 \right] - 5 \text{ dB} \quad [Eq 41]$$

This is simplified, because the 2<sup>nd</sup> term is usually much larger than 1, to:

$$TL = 10 \log_{10} \left[ \frac{\pi M_s f}{Z_{air}} \right]^2 - 5 \text{ dB} \quad [Eq 42]$$

An alternate form that is written by the author for equation [37] is:

$$TL = 20 \log_{10} M_s + 20 \log_{10} f - 20 \log_{10} \frac{Z_{air}}{\pi} - 5 \text{ dB} \quad [Eq 43]$$

To transition from region II to region III, the author introduces a segment as a plateau that is given in the following table, each material having its respective plateau value and spread.

| Material | $TL_p, \text{dB}$ | $\Delta f_p = f_{1p} - f_{2p}$ | Octaves $f_{2p}/f_{1p}$ |
|----------|-------------------|--------------------------------|-------------------------|
| Brick    | 37                | 2.2                            | 4.5                     |
| Concrete | 38                | 2.2                            | 4.5                     |

Table 2 - Reference information for the plateau area for the 1<sup>st</sup> prediction method

### Region III

For frequencies, greater than the critical frequency, the author cites Beranek:

$$TL = TL_n(f_c) + 10 \log_{10}(\eta) + 33.22 \log_{10}(f/f_c) - 5.7 \text{ dB} \quad [Eq 44]$$

Where  $TL_n(f_c)$  is equal to:

$$TL_n(f_c) = 10 \log_{10} \left[ 1 + \left( \frac{\pi M_s f_c}{Z_{air}} \right)^2 \right] \text{ dB} \quad [Eq 45]$$

Where  $f_{2p} = \text{octaves} \left( \frac{f_2}{f_1} \right) * f_{1p}$  given by the table above.

$$TL = TL_p + 33.22 \log_{10} \left( \frac{f}{f_{2p}} \right) \text{ dB} \quad [Eq 46]$$

### 2.1.2.3 A more intricate method that takes into account different variables as it builds the transmission loss curve.

For a homogeneous wall the sound transmission loss is given by the behavior of the frequency in three different ranges as established by the stiffness, mass and damping controlled regions.

#### Region I – Stiffness controlled region

In this region, the mechanical compliance  $C_s$  of the wall/partition is used to obtain the sound power transmission coefficient. The stiffness of the partition is the primary means of calculating the sound transmission and for that reason the mechanical compliance, taken as the reciprocal of the spring constant, is obtained for a rectangular panel with the following expression:

$$C_s = \frac{768(1-\sigma^2)}{\pi^8 E h^3 \left(\frac{1}{a^2} + \frac{1}{b^2}\right)^2} \quad [Eq 47]$$

Leading to a new definition of the sound power transmission coefficient as,  $K_s$  :

$$K_s = 4\pi Z_{air} C_s f \quad [Eq 48]$$

Allowing for the calculation of the transmission loss with:

$$TL = 20 \log_{10} \left(\frac{1}{K_s}\right) \text{ dB} \quad [Eq 49]$$

### Region II – Mass controlled region

The plate dimensions are directly related to the resonance frequency,  $f_{m,n}$ , which determine when region I has been surpassed and the affecting behavior is now that of region II. For this purpose, the first resonant frequency is calculated using the longitudinal wave speed,  $C_L$ :

$$C_L = \sqrt{\left[\frac{E}{\rho_w(1-\sigma^2)}\right]} \text{ m/s} \quad [Eq 50]$$

$$f_{m,n} = \left(\frac{\pi}{4\sqrt{3}}\right) C_L h \left[\left(\frac{m}{a}\right)^2 + \left(\frac{n}{b}\right)^2\right] \text{ Hz} \quad [Eq 51]$$

Where  $a$  and  $b$  stand for the dimensions of the panel and  $m$  and  $n$  stand for integer values.

For each frequency, now one can obtain the transmission loss via normal incidence:

$$TL_n = \log_{10} \left(1 + \frac{\pi f M_s}{Z_{air}}\right) \text{ dB} \quad [Eq 52]$$

And using this transmission loss at normal incidence, a user can find:

$$TL = TL_n - 5 \text{ dB} \quad [Eq 53]$$

This behavior ends with the transition to region III, when the critical frequency is overtaken:

$$f_c = \frac{\sqrt{3}c^2}{\pi C_L h} \text{ Hz} \quad [Eq 54]$$

This reinforcement between the incident sound wave and the bending wave first occurs at grazing incidence of  $90^\circ$  as mentioned by the author Randall F. Barron.

### Region III – Damping controlled region

Using the internal damping of the material and the frequency of the incident sound, for random incidence we get:

$$TL_{fc} = 10 \log_{10} \left( 1 + \left( \frac{\pi M_s f_c}{Z_{air}} \right)^2 \right) \text{ dB} \quad [Eq 55]$$

Defining  $TL_{fc}$  as the transmission loss for the critical frequency, the transmission loss is given by:

$$TL = TL_{fc} + 10 \log_{10}(\eta) + 33.22 \log_{10} \left( \frac{f}{f_c} \right) - 5.7 \text{ dB} \quad [Eq 56]$$

For double leaf structures, the author Randall F. Barron presents one model for transmission loss predictions.

#### 2.1.2.4 Composite Wall with an Airspace Transmission Loss

The double leaf construction is made up of two panels separated by an air gap and is commonly used for transmission loss purposes as mentioned by the author Randall F. Barron. In figure 4 there are two examples of double leaf structures.

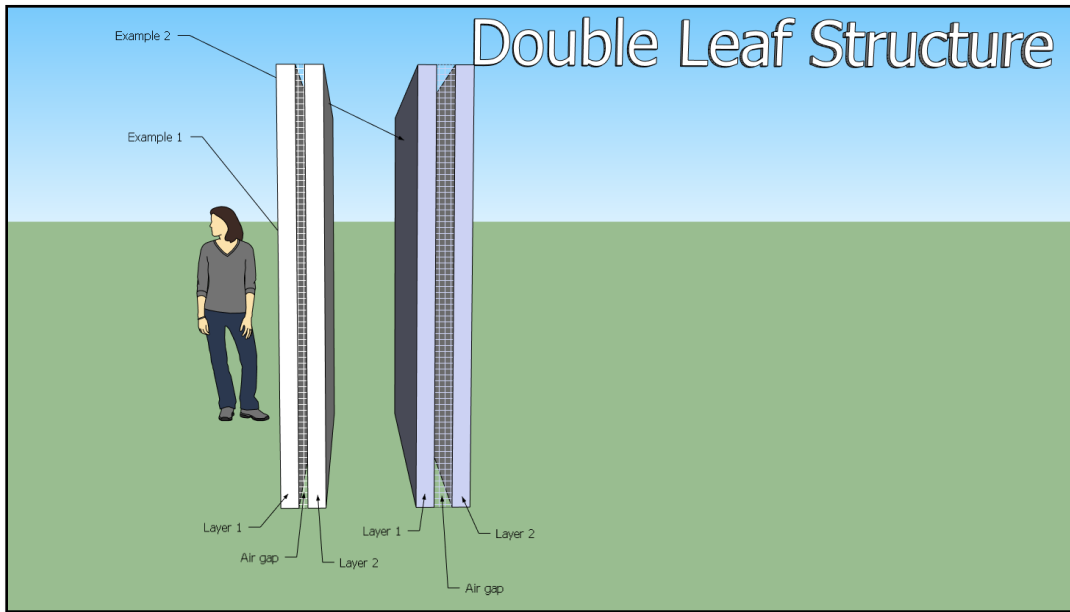


Figure 4 – Examples of a double leaf structure

For this type of construction, the use of a resonant frequency given by the air cavity of the double leaf panel,  $f_0$ , is determined with:

$$f_0 = \frac{c_{air}}{\pi} \left[ \frac{\rho}{d} \left( \frac{1}{M_{S1}} + \frac{1}{M_{S2}} \right) \right] \text{ Hz} \quad [Eq 57]$$

With the use of the resonant frequency given by the air cavity of the double leaf panel, the author Randall F. Barron creates a transition between two regimes. Regime A and Regime B are defined with the resonant frequency of the air cavity,  $f_0$ :

When the following condition is met:

$$\frac{Z_{air}}{\pi(M_{s1} + M_{s2})} < f < f_0$$

The transmission loss is determined by behavior in regime A:

$$TL = 20 \log_{10}(M_{s1} + M_{s2}) + 20 \log_{10}(f) - 47.3 \text{ dB} \quad [Eq 58]$$

When the frequency exceeds the resonant frequency of the cavity the behavior is now represented by regime B, in other words:

$$f_0 < f < \frac{c_{air}}{2\pi d}$$

The transmission loss in this regime is given by:

$$TL = TL_1 + TL_2 + 20 \log_{10} \left( \frac{4\pi f d}{c_{air}} \right) \text{ dB} \quad [Eq 59]$$

The Transmission loss values for  $TL_1$  and  $TL_2$  are those for each independent layer and  $d$  stands for the distance of the air gap between both layers as can be seen in Figure four.

The final regime given by the author Randall F. Barron is regime C, and it is used when the following condition is met:

$$f > \frac{c}{2\pi d}$$

The transmission loss in this regime is given by:

$$TL = TL_1 + TL_2 + 10 \log_{10} \left( \frac{4}{1 + \left(\frac{2}{\alpha}\right)} \right) \text{ dB} \quad [Eq 60]$$

Having  $\alpha$  as the surface absorption coefficient for the panels.

### 2.1.2.5 Multilayer Structure

For a multilayer structure composed of two laminate layers, the following definitions are applied by the author Randall F. Barron to the bending stiffness which is mentioned as the flexural rigidity:

$$B = \frac{E_1 h_1^3}{12(1 - \sigma_1^2)} \left[ 1 + 3 \left( 1 - \left( \frac{2X}{h_1} \right) \right)^2 \right] + \frac{E_2 h_2^3}{12(1 - \sigma_2^2)} \left[ 1 + 3 \left( 1 + \frac{2X}{h_2} \right)^2 \right] \quad [Eq 61]$$

Where the distance to the neutral axis X is given as:

$$X = \frac{E_1 h_1^2 - E_2 h_2^2}{2(E_1 h_1 + E_2 h_2)} \quad m \quad [Eq 62]$$

And effective damping coefficient is given by:



$$\eta = \frac{(\eta_1 E_1 h_1 + \eta_2 E_2 h_2)(h_1 + h_2)^2}{E_1 h_1^3 [1 + 3(1 - 2X/h_1)^2] + E_2 h_2^3 [1 + 3(1 + 2X/h_2)^2]} \quad [\text{Eq 63}]$$

Allowing the user to calculate the critical frequency,  $f_c$ , of the multilayered structure with its effective mass,  $M$ , using the following definitions:

$$M = \rho_1 h_1 + \rho_2 h_2 \quad [\text{Eq 64}]$$

$$f_c = \frac{c_{\text{air}}^2}{2\pi} \left(\frac{M}{B}\right)^{1/2} \text{ HZ} \quad [\text{Eq 65}]$$

### 2.1.3 Architectural Acoustics – Marshall Long

This is a brief summary from chapter 9 sound transmission loss (Long, n.d.).

#### 2.1.3.1 Transmission Loss Theory

The general transmission loss for normal incidence is given by:

$$TL_n = 10 \log_{10} \left( \left[ 1 + \left( \frac{\zeta_n \cos(\theta)}{2} \right)^2 \right] \right) \text{ dB} \quad [\text{Eq 66}]$$

Where the normalized panel impedance  $\zeta_n$  is given by:

$$\zeta_n = \frac{Z_n}{Z_{\text{air}}} \quad [\text{Eq 67}]$$

And the panel impedance  $Z_n$  is defined as:

$$Z_n = j\omega M_s \quad [\text{Eq 68}]$$

Equation [56] is presented as the mass law by Marshall Long.

To calculate the coincidence frequency the author states that it varies with the angle of incidence and gives the following expression to calculate the frequency at which coincidence occurs,  $f_{co}(\theta)$ :

$$f_{co}(\theta) = \frac{c_{\text{air}}^2}{2\pi \sin^2(\theta)} \sqrt{\frac{M_s}{B}} \text{ HZ} \quad [\text{Eq 69}]$$

The critical frequency is defined as the minimum value for the matching frequency at grazing incidence,  $f_c$ , and it is calculated with:

$$f_c = \frac{c_{\text{air}}^2}{2\pi} \sqrt{\frac{M_s}{B}} = \frac{c_{\text{air}}^2}{2\pi h} \sqrt{\frac{12(1-\sigma^2)\rho_m}{E}} \text{ HZ} \quad [\text{Eq 70}]$$

Where the angle of incidence  $\theta$  is used to create the following relation:

$$f_{co}(\theta) = \frac{f_c}{\sin^2(\theta)} \text{ HZ} \quad [\text{Eq 71}]$$

### 2.1.3.2 Single Panel Transmission Loss

When:

$$f \leq \frac{f_c}{2}$$

The transmission loss is given by:

$$TL = 20 \log_{10}(fM_s) - 47.3 \text{ dB [Eq 72]}$$

Marking one of the first regions defined by the use of the critical frequency,  $f_c$ .

When:

$$f > \frac{f_c}{2} \text{ and } f < f_c$$

The transmission loss is determined with:

$$TL = 10 \log_{10} \left( 1 + \left( \frac{Bk^4 \sin^4(\theta) \cos(\theta)}{2Z_{air}\omega} \right)^2 \right) \text{ dB [Eq 73]}$$

Defining the bending stiffness  $B$  as:

$$B = \frac{Eh^3}{12(1-\sigma^2)} \text{ [Eq 74]}$$

And  $k$  as the wave number vector:

$$k = \frac{2\pi}{\lambda} = \frac{\omega}{c_{air}} \text{ [Eq 75]}$$

When:

$$f > f_c$$

The transmission loss is given by:

$$TL = 20 \log_{10} \left( \frac{\omega M_s}{2Z_{air}} \right) + 10 \log_{10} \left( \frac{2\eta}{\pi} \left( \frac{f}{f_c} - 1 \right) \right) \text{ dB [Eq 76]}$$

Where  $\Delta f = 0.236$  for 1/3 octave bands and  $\Delta_b = 0.707$  for octave bands.

When:

$$f = f_c$$

The transmission loss is given by:

$$TL = 20 \log_{10} \left( \frac{\omega_c M_s}{2Z_{air}} \right) + 10 \log_{10} \left( \frac{2\eta \Delta f}{\pi f_c} \right) \text{ dB [Eq 77]}$$

### 2.1.3.3 Double Leaf Transmission Loss

For double leaf structures the air cavity again will behave like a spring and as such there will be a mass-air-mass resonance at a given frequency:

$$f_0 = \frac{1}{2\pi} \sqrt{\frac{3.6\rho_{air}c_{air}^2}{M'd}} \text{ Hz} \quad [Eq 78]$$

Where  $M'$  stands for the effective mass per unit area of the type of construction defined as:

$$M' = \frac{2M_{s1}M_{s2}}{M_{s1}+M_{s2}} \quad [Eq 79]$$

And  $d$  is the distance of the air gap between both layers.

Considering this, there are two prediction schemes for double leaf structures.

The first is given by a transmissivity coefficient:

$$\tau_\theta = [1 + (X_1 + X_2) + (1 - e^{-j\sigma})] \quad [Eq 80]$$

Where the use of the impedances is established with:

$$X = \frac{Z_n \cos(\theta)}{2Z_{air}} \quad [Eq 81]$$

and  $\sigma$  is a function of the wave number vector:

$$\sigma = 2kd \cos(\theta) \quad [Eq 82]$$

The transmission loss is given by:

$$TL = 10 \log_{10}(\tau_\theta) \text{ dB} \quad [Eq 83]$$

The second prediction scheme is the following:

For frequencies that are above the mass-air-mass resonance frequency,  $f_0$  in other words:

$$f_0 < f$$

The transmission loss is given by:

$$TL = 10 \log_{10} \left( 1 + \left( \frac{\omega M}{3.6Z_{air}} \right)^2 \right) \text{ dB} \quad [Eq 84]$$

For any frequency above the mass-air-mass resonance and below the limiting frequency, in other words:

$$f_0 \leq f < f_l$$

Then its transmission loss is determined by:

$$TL = 20 \log_{10} \left( \frac{\omega^2 M_{s1} M_{s2}}{(3.6Z_{air})^2} 2kd \right) \text{ dB} \quad [Eq \ 85]$$

The final range defined by the author Marshall Long is when the limiting frequency is surpassed, in other words:

$$f > f_l$$

The transmission loss in this range is defined by:

$$TL = TL_3 + TL_2 + 6 \text{ dB} \quad [Eq \ 86]$$

## 2.1.4 Accuracy of Prediction Methods for Sound Transmission Loss

This is a brief summary of the article (Ballagh, 2004) presented in the 33<sup>rd</sup> international congress and exposition on noise control engineering titled “Accuracy of Prediction Methods for Sound Transmission Loss” that shows different methods for predicting sound transmission loss for walls. For the purpose of simplicity, the single leaf and ideal double leaf walls will be presented from the article.

### 2.1.4.1 Single Leaf Transmission Loss

The mass law is presented as:

$$TL = 20 \log_{10}(M_s f) - 47 \text{ dB} \quad [Eq \ 87]$$

A modification is introduced to the mass law as follows:

$$TL = 20 \log_{10}(M_s f) - 10 \log_{10} \left( \frac{2\eta w}{\pi w_c} \right) - 47 \text{ dB} \quad [Eq \ 88]$$

The purpose of this change is to account for the critical frequency behavior in the transmission loss. A third equation offered for transmission loss is given to consider the surface area of the panel which affects the forced waves radiation efficiency:

$$\Delta R = -\log_{10}[\log(kA^{1/2})] + 20 \log_{10} \left[ 1 - \left( \frac{w}{w_c} \right)^2 \right] \text{ dB} \quad [Eq \ 89]$$

As stated by the author, these expressions are used only for thin panels because of shear waves and its effect of reducing the transmission loss. The author mentions that this attenuation is present at high frequencies and its curve reduces from a 12 dB/octave to 6 dB/octave rate.

### 2.1.4.2 Double Leaf Transmission Loss

The simplest case for a double leaf structure can be considered as two thin panels separated by an air gap filled with acoustical absorbent material with no inter connections between the two panels.

The analytical model presented in this article for double leaf walls produces predictions for three different frequency ranges using the mass air mass resonance frequency and the limiting

frequency to represent changes in the transmission loss dependent of the cavity and structure dimensions.

The first range is established with:

$$f < f_0$$

The transmission loss in this range is given by:

$$TL = 20 \log_{10}(f(M_{s1} + M_{s2})) - 47 \text{ dB} \quad [\text{Eq } 90]$$

For the second range, we get that, when:

$$f_0 < f < f_l$$

The transmission loss is determined with:

$$TL = TL_1 + TL_2 + 20 \log_{10}(fd) - 29 \text{ dB} \quad [\text{Eq } 91]$$

For the third range, the final range:

$$f_l < f$$

The transmission loss is given by:

$$TL = TL_1 + TL_2 + 6 \text{ dB} \quad [\text{Eq } 92]$$

### 2.1.5 The Transmission Loss of Multilayer Structures

Using a random incidence average transmission coefficient, the author defines TL as:

$$TL = -10 \log_{10}[T^2] \text{ dB} \quad [\text{Eq } 93]$$

To obtain this T coefficient, we must define the bending impedance.

$$Z_B = i\{-m\omega + Bk_x^4/\omega\} \quad [\text{Eq } 94]$$

As well as the extensional impedance.

$$Z_E = \frac{-i4\rho C_s^2}{\omega h(1-\sigma)} \left\{ \frac{2k_x^2 - (1-\sigma)\omega^2/C_s^2}{k_x^2 - \omega^2/C_s^2} \right\} \quad [\text{Eq } 95]$$

So, that we may find an estimate to express a thin panel.

$$C = \frac{1}{[1+Z_B \cos \theta / 2Z_{air}][1-Z_E \cos \theta / 2Z_{air}]} \quad [\text{Eq } 96]$$

The letter  $C$  represents a type of arbitrary constant.

$$R = -C(1 + Z_B Z_E \frac{\cos^2 \theta}{4Z_{air}^2}) \quad [\text{Eq } 97]$$

$$T = -C(Z_B + Z_E) \cos \theta / 2Z_{air} \quad [\text{Eq } 98]$$

Where R and T are the reflection and transmission coefficient.

Defining  $k_x$  as a speed propagation constant in x direction and  $k_y$  as another speed propagation constant in y direction.

The velocity of compressional waves and shear waves are given by the variables describing the properties of the panel and can be calculated with the following equations:

$$C_c = \sqrt{\frac{E(1-\sigma)}{\rho(1+\sigma)(1-2\sigma)}} \quad \text{Eq 99}$$

$$C_s = \sqrt{\frac{E}{2\rho(1+\sigma)}} \quad \text{Eq 100}$$

Another definition given to the bending and extensional impedances is:

$$Z_B = \frac{i8\rho_{air}C_s^4}{\omega^3} \left\{ \beta k_x^2 \tanh\left(\frac{\beta h}{2}\right) - \left(k_x^2 - \frac{\omega^2}{2C_s^2}\right)^2 \frac{\tanh\left(\frac{\alpha h}{2}\right)}{\alpha} \right\} \quad [\text{Eq 101}]$$

$$Z_E = \frac{iZ_{air}\rho C_s^4}{\omega^3} \left\{ -\beta k_x^2 \coth\left(\frac{\beta h}{2}\right) + \left(k_x^2 - \frac{\omega^2}{2C_s^2}\right)^2 \frac{\coth\left(\frac{\alpha h}{2}\right)}{\alpha} \right\} \quad [\text{Eq 102}]$$

Where  $\beta$  and  $\alpha$  are defined as:

$$\alpha^2 = k_x^2 - \frac{\omega^2}{C_c^2} \quad [\text{Eq 103}]$$

$$\beta^2 = k_x^2 - \frac{\omega^2}{C_s^2} \quad [\text{Eq 104}]$$

## Chapter III

### 3.1 ISO 16283 “Field Measurement of Sound Insulation in buildings and of building elements” Part 1 Airborne sound insulation

This summary provides information that was selected and used from the ISO 16283 standard. The low frequency procedure has been omitted because it was not deemed to be pertinent to the case in study, reasoning that the low frequency procedure needs to be implemented in rooms that are inferior in volume to 25 m<sup>3</sup>. The purpose of using this ISO 16283 standard is to obtain transmission loss data that can be used to apply the ISO 717-1 standard.

The standard gives the details of a procedure for field measurement of sound insulation in buildings, focusing mainly on airborne sound insulation. ISO 16283 is an update to the ISO 140 series which lacked clarity in specifying if the operators could be present during the measurements in the room, and that it was intended for measurements in diffuse sound fields, or those that could be approximated to it. With the latter in mind, the ISO 16283 standard applies to rooms that have a sound field that can be or cannot be considered a diffuse sound field. It also clarifies how an operator can measure the sound field by being present in the room by keeping his/her trunk at an arm’s length from the fixed microphone, and includes additional guidance which the ISO 140 series lacked in the ISO 140-4 standard for airborne sound insulation between rooms. The intended room volumes for the standard vary from 10 [m<sup>3</sup>] to 250 [m<sup>3</sup>] and its frequency range lies in the 50 [Hz] to 5 [kHz] range. The results can be used to quantify or assess an unfurnished/furnished room measuring the airborne sound insulation whether the sound field is or is not approximated to a diffuse sound field. The results of the measurement are frequency dependent and can be converted using the ISO 717-1 standard into a single number quantity characterizing the acoustic performance of the test element. ISO 16283 introduces the energy-average sound pressure level in a room as  $L$  and expresses it in dBs, the reverberation time as the time required for there to be a 60 [dB] decrease in the sound pressure level in a room after the sound source has ceased and is expressed in seconds. The background noise level is the measured sound pressure level when the main source is off and all other sources are operating in the room. The definition for a partition is the total surface of the common or separating wall between the receiving and source test rooms. The level difference is the energy-average sound pressure level difference between the receiving and source rooms with an operating loudspeaker in the source room (“BSI Standards Publication Acoustics — Field measurement of sound insulation in buildings and of building elements Part 1 : Airborne sound insulation,” 2014).

$$D = L_1 - L_2 \quad [Eq\ 105]$$

$L_1$  represents the sound pressure level in the source room.

$L_2$  represents the sound pressure level in the receiving room.

Using the level difference  $D$ , the standardized level difference ( $D_{nT}$ ) can be calculated:

$$D_{nT} = D + 10 \log_{10} \frac{T}{T_0} \quad [Eq\ 106]$$

Defining  $T$  as the reverberation time in the receiving room and  $T_0$  as the reference reverberation time, taken as 0.5 [s] for residences. The level difference  $D$  can also be used to calculate the

apparent sound reduction index  $R'$  by using the area of the common partition and the equivalent absorption area of the receiving room, again where  $S$  is the former and  $A$ , the latter.

$$R' = D + 10 \log_{10} \frac{S}{A} \quad [Eq\ 107]$$

The laboratory measurement of the sound reduction index  $R$  can be compared to the apparent sound reduction index  $R'$  field measurement and will show a higher relation to the subjective impression of airborne sound insulation than the  $D_{nT}$  standardized level difference.

The equivalent absorption area,  $A$ , in the receiving room, is calculated using Sabine's formula with the reverberation time and the volume of the receiving room.

$$A = \frac{0.16V}{T} \quad [Eq\ 108]$$

In the calibration step the correction factor cannot exceed 0,5 [dB]. Some other requirements by the standard include that one room is chosen as the source room and another as the receiving room, the former having the source/loudspeaker. It establishes the default procedure for all frequencies using a fixed microphone moved from one position to another although this is not the only option. The measurements should take place in the central zone of the room at positions away from the room boundaries. It also mentions that sound fields in typical rooms will not always behave like a diffuse sound field over the entire frequency range and that the default procedure allows for the measurements to be taken without this approximation.

The default procedure uses the measurements to determine the average sound pressure level in the central zone of both the source and the receiving rooms with the source on and when the source is off it uses the background noise level in the receiving room. A consideration for the sound power of the source/loudspeaker is that it should be sufficiently high for the sound pressure level in the receiving room to be higher than the measured background noise level. For the default procedure, it is stated that the background noise level shall be at least 6 [dB] lower than the level combination in each frequency band of both the signal and background noise. If the difference is greater than 6 [dB] but lower than 10 [dB] the corrections done to the energy average sound pressure level use the following formula:

$$L = 10 \log_{10}(10^{L_{sb}/10} - 10^{L_b/10}) \quad [Eq\ 109]$$

$L_{sb}$  represents the level of the signal plus the background noise.

$L_b$  represents the level of the background noise.

For the broadband signal to be used the standard recommends the use of white or pink noise but cautions that the energy average sound pressure levels in the source room should not have a difference in level of more than 8 [dB] between adjacent 1/3 octave bands when analyzing above 100[ Hz]. Considering the use of a single loudspeaker in the source room, it is stated that a minimum of 5 positions should be used in each room for each loudspeaker position. After measuring the sound pressure levels in the source and receiving room, the energy average sound pressure level can now be calculated for each room (source and receiving) which in turn leads to the calculation of the standardized level difference and the apparent sound reduction index. This



process is repeated for each loudspeaker position and accordingly a  $D_{nT}$  is calculated to represent the different loudspeaker positions with the following formula:

$$D_{nT} = 10 \log_{10} \frac{1}{m} \sum_{j=1}^m 10^{-D_{nT,j}/10} \quad [\text{Eq 110}]$$

At the same time, the apparent sound reduction index accounting for the different number of loudspeaker positions can be calculated with:

$$R' = -10 \log_{10} \frac{1}{m} \sum_{j=1}^m 10^{-R'_j/10} \quad [\text{Eq 111}]$$

The letter m stands for the number of loudspeaker positions.

After stating the information for the loudspeaker, the standard now moves on to give details for the distances for each microphone position and the averaging time for different frequency ranges.

Between fixed microphone positions the minimum distance will be 0.7 [m]. For any microphone position and a room boundary, the minimum distance will be 0.5 [m]. Finally, any microphone position will be at a distance of 1[m] from the loudspeaker. The averaging time for the different frequency ranges are given in table 2. Table 3 shows the center frequency of the 1/3 octave bands in the frequency range column. The total range covered goes from 50 [Hz] to 5 [kHz]

| Time [s]       | Frequency range [Hz] |
|----------------|----------------------|
| 6              | 100 – 400            |
| No less than 4 | 500-5000             |
| At least 15    | 50 – 80              |

Table 3 - Averaging times/ Frequency Range

To calculate the energy-average sound pressure level for the microphone positions after finding the pressure value for each point, the standard uses the following formula:

$$L = 10 \log_{10} \frac{(P_1^2 + P_2^2 + \dots + P_n^2)}{nP_0^2} \quad [\text{Eq 112}]$$

For an easier and more direct way to calculate the energy-average sound pressure level using the sound pressure level measurements:

$$L = 10 \log_{10} \frac{1}{n} \sum_{i=1}^n 10^{L_i/10} \quad [\text{Eq 113}]$$

Where n stands for the number of different microphone positions.

### 3.2 ISO 717-1 “Rating of sound insulation in building and of building elements – Part 1 Airborne Sound Insulation”

The goal of this standard is to normalize the frequency dependent airborne sound insulation into a single number rating that uses that relationship to characterize its acoustic properties. Some of the global values used for evaluation of airborne sound insulation in buildings and of building elements such as walls, floors, doors, and windows are:

- the normalized level difference -  $D_n$ ,
- the weighted normalized level difference –  $D_{n,w}$
- the Standardized level difference -  $D_{nT}$ ,
- the weighted standardized level difference –  $D_{nT,w}$ ,
- the sound reduction index -  $R$ ,
- the weighted sound reduction index -  $R_w$ ,
- the apparent sound reduction index -  $R'$ ,
- the weighted apparent sound reduction index –  $R'_w$ ,

Where some of these are obtained by following the procedures established in the ISO 16283 standard. By using the results obtained in the measurements, and comparing them to reference values in 1/3 octave bands or in octave bands, the global value is obtained. Table 3 depicts the 1/3 octave sound insulation reference values given by the ISO 717-1.

| [Hz] | 100 | 125 | 160 | 200 | 250 | 315 | 400 | 500 | 630 | 800 | 1000 | 1250 | 1600 | 2000 | 2500 | 3150 | 4000 | 5000 |    |
|------|-----|-----|-----|-----|-----|-----|-----|-----|-----|-----|------|------|------|------|------|------|------|------|----|
| [dB] | 33  | 36  | 39  | 42  | 45  | 48  | 51  | 52  | 53  | 54  | 55   | 56   | 56   | 56   | 56   | 56   | 56   | 56   | 56 |

Table 4 - Sound insulation reference values ISO 717-1

The comparison method consists in displacing the ISO 717-1 reference curve in steps of 1 [dB] towards the calculated curve from the measurement and getting to the highest unfavorable deviation value without exceeding 32 [dB] for 1/3 octave bands or 10[dB] for octave bands. This unfavorable deviation is caused when the measured values of the curve are below the reference curve. For the spectrum adaptation terms, which are used to factor in different types of source spectra,  $C$  and  $C_{tr}$ , reference values are given in table 4.

| [Hz]          | 50  | 63  | 80  | 100 | 125 | 160 | 200 | 250 | 315 | 400 | 500 | 630 | 800 | 1K  | 1250 | 1600 | 2k  | 2.5k | 3150 | 4k  | 5k  |     |
|---------------|-----|-----|-----|-----|-----|-----|-----|-----|-----|-----|-----|-----|-----|-----|------|------|-----|------|------|-----|-----|-----|
| $C$ [dB]      | -40 | -36 | -33 | -29 | -26 | -23 | -21 | -19 | -17 | -15 | -13 | -12 | -11 | -10 | -9   | -9   | -9  | -9   | -9   | -9  | -9  | -9  |
| $C_{tr}$ [dB] | -25 | -23 | -21 | -20 | -20 | -18 | -16 | -15 | -14 | -13 | -12 | -11 | -9  | -8  | -9   | -10  | -11 | -13  | -15  | -16 | -18 | -18 |

Table 5 - Adaptation Terms ISO 717-1

Given the reference values, the adaptation terms can be calculated with:

$$C_j = X_{Aj} - X_w \quad [Eq 114]$$

Where  $X_{Aj}$  is given by:

$$X_{Aj} = -10 \log_{10} \sum 10^{(L_{ij}-X_i)/10} \quad [Eq 115]$$

$X_w$  is calculated using the procedure of displacing the measured curve towards the reference curve using  $R, R', D_{nT}, D_n$  giving the user a global index value. After calculating  $X_w$  the variable  $X_{Aj}$  is determined using the apparent sound reduction index, sound reduction index, normalized level difference or the standardized level difference to characterize the difference between the A weighted sound level difference in the source and receiver room for white noise as  $X_i$  and  $L_{ij}$  are the reference values for the spectrum sound level of each adaptation term. It is important to note that the C adaptation term is used for pink noise weighted in A and that there is no uncertainty value by itself.

## Chapter IV: Research Focus

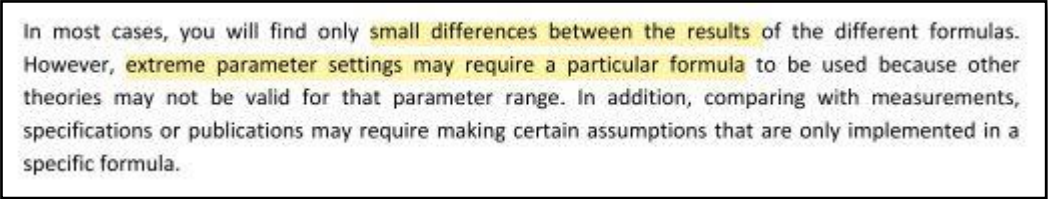
### 4.1 Research Line

The research line for this project is applied acoustics and its purpose is to set up an exploration into different theories available for sound insulation prediction models used for airborne noise transmission.

### 4.2 Data gathering techniques

#### 4.2.1 User Manual Key information (SoundFlow)

The Graphical user interface as mentioned in the user manual, is said to be designed so that a user can have an easy and intuitive way of defining a structure that can be composed of multiple layers and a display of the results that is easy to understand. For this purpose, the designers gave the user the ability to customize the appearance of the interface and even included several shortcut keystroke combinations to optimize its use. Some of the indices and ratings that are given in the results display section are  $R_w$  and STC, among others ( $NRC$ ,  $\alpha_w$ ,  $C$ ,  $C_{tr}$ ) and these are the broadband quantities calculated by the program. They mention a warning for the rigid back selection since this can interfere with the TL prediction by not calculating a transmission factor for the reflection coefficient is 1 (Ahnert, Media, & Ease, 2011). The user can define the dimensions of the structure that he/she is going to work with and the program uses those dimensions to compute the result that is equivalent to a measurement in the reverberation room with a sample of the same size. The different physical theories used to determine the different calculation formulas can be changed by using the absorber model parameter where the equivalent calculation formulas are those by Bies.



In most cases, you will find only small differences between the results of the different formulas. However, extreme parameter settings may require a particular formula to be used because other theories may not be valid for that parameter range. In addition, comparing with measurements, specifications or publications may require making certain assumptions that are only implemented in a specific formula.

*Screenshot 1– SoundFlowUserManual*

The Bies model is referenced to the “Engineering Noise Control Theory and Practice, third edition” book. As for transmission loss, it is defined as a common quantity that is used to describe the acoustic insulation of structures. It states two ways of specifying transmission loss. One uses the sound power and the other uses sound pressure.

#### 4.2.2 User Manual Key information (dBKAisla)

The user manual warns that it is the user's responsibility to decide whether he/she has the necessary theoretical knowledge to use the program correctly and the company bears no liability for any damage arising from the inadequate use by people not practicing in its technical department. One of the purposes of this program is to study sound insulation by use of the calculations for single and multiple walls. Some of the broadband quantities displayed by the program are  $R_A$  and  $R_w$  ( $C$ ;  $C_{tr}$ ). For double leaf panels it is mentioned that the cavity is filled 50% with absorbent material.

Mass Law – opposes incident acoustic energy through its mechanical inertia, resisting/holding back vibrations. This means to say that the mass law only takes into account the surface of the mass wall.

Corrected Mass Law – Makes use of the coincidence frequency, surface mass, damping coefficient and wall surface. The difference from the mass law is that, its slope now varies according to different regions established by the coincidence frequency.

1<sup>st</sup> Region – located below the coincidence frequency and it has a slope of 6 [dB] per octave

2<sup>nd</sup> Region – located in the range of  $f_c$  where the coincidence phenomenon takes place.

3<sup>rd</sup> Region – located above  $f_c$  taking a slope of 9 [dB] per octave.

Multiple walls – The parameter to define the behavior for this type of construction is used as the resonance frequency, aiming for it to be as low as possible. The empirical formulas by Sewell, Cremer and Sharp are used for all the type of construction elements and there are no references in the user manual.

#### 4.2.3 Common Ground

Broadband quantities and results sheet.

## Chapter V: Engineering Development

Chapter V: Engineering development will give a description of the process and steps taken, to accomplish the research objective in this thesis work.

### 5.1 Methodology

#### 5.1.1 Choosing software

The first decision for this project was choosing the software that would be used as a reference to compare single number ratings,  $R_w(C, C_{tr})$ . To do so, these were the minimum requirements for the software to be eligible:

- ✓ Runs in OS Windows 10/8
- ✓ Prints out a report sheet for airborne sound
- ✓ Uses graphs and tables to display results
- ✓ Calculates a single number rating for airborne sound
- ✓ It is a demo version
- ✓ Allows user input for new materials

Two software will be chosen for the sake of simplicity as well as budget limitations, hence the demo version requirement. The software user input and result sheets may vary according to software but using the parameters that are similar or the same, will enable a quick evaluation/comparison between their functioning. Also, the difference in the results delivered by each software will show what each company finds some information more pertinent than other when dealing with TL reports.

#### 5.1.2 Revising Literature

To define the different types of structures that will be worked on, the literature is revised. As can be seen in the theoretical framework and state of the art. In regard to the materials, that will be used to model the different types of structures, brick and concrete will be chosen because they are considered as heavyweight construction materials. Heavyweight materials are chosen because some models are said to not work well (Cambridge, 2012) with those types of materials. Table 6 shows the solid plate properties for the chosen materials representing heavyweight materials.

Table 6 – Solid Plate Properties

| Material    | Density<br>$\left[\frac{kg}{m^3}\right]$ | Young's<br>modulus<br>$[GPa]$ | Poisson's<br>ratio | Loss<br>Factor |
|-------------|--|-------------------------------|--------------------|----------------|
| Concrete    | 2000                                     | 15                            | 0.24               | 0.03           |
| Solid Brick | 1800                                     | 16                            | 0                  | 0.03           |

In the literature revision, it becomes evident that the structures that are well documented are the single leaf, double leaf and multilayer structure defined as two layers on top of each other. To this end, the structures chosen to work on are those that can be accommodated in the simplest case of sound insulation such as the single leaf, double leaf and multilayer

element which were mentioned above. In regard to the dimensions of the element/structure found in the literature revision, it is found that thick panels are considered to have discrepancies in the predictions by different models used. Considering these discrepancies, the elements are focused on structures that can be considered as thin panels. This is done so by limiting the structure thickness to no more than thirty centimeters.

### **5.1.3 Construction of Sample size**

To analyze the different models and use descriptive statistics, some authors (Kurra, 2012) have used sample sizes of 65 cases to look at the results and from them conclude something about the total population. Considering this, over 60 cases were carried out and studied. To not give too much information where some of it may become redundant, the 30 most representative cases of the study will be presented and analyzed.

### **5.1.4 Process to accomplish an analysis of the models used in sound insulation predictions tools like SoundFlow and dBKAisla for single, double and multilayer structures.**

In order to examine methodically the different prediction models used for sound insulation in private software, the following sequence of steps is presented.

The first step is to generate TL predictions for single leaf, double leaf and multilayer element structures that are displayed in Table 7 which also gives the total number of cases analyzed in this project.

Using the predictions in Table 7 as a reference for the transmission loss, the second step will be to review the authors cited in the user manuals. Descriptive statistics will be used to analyze the different models and the prediction values from each software to defend a hypothesis. The final step, fourth, consists in comparing the predictions of the software to the reviewed literature values.

Table 7 – Single Leaf, Double Leaf [ML: Model0 dBKAisla; CML:Model1 dBKAisla; BIS Model2 SoundFlow]

| Case #  | [Material; Thickness;(dimensions) Type of structure; Model] | [Software] |
|---------|---|------------|
| Case 1  | Concrete 10 [cm] Single leaf structure ML                   | dBKAisla   |
| Case 2  | Concrete 25 [cm] Single leaf structure ML                   | dBKAisla   |
| Case 3  | Concrete 30 [cm] Single leaf structure ML                   | dBKAisla   |
| Case 4  | Brick 10 [cm] Single leaf structure ML                      | dBKAisla   |
| Case 5  | Solid Brick 25 [cm] Single leaf structure ML                | dBKAisla   |
| Case 6  | Solid Brick 30 [cm] Single leaf structure ML                | dBKAisla   |
| Case 7  | Concrete 5 [cm] Single leaf structure BIS                   | SoundFlow  |
| Case 8  | Concrete 10 [cm] Single leaf structure BIS                  | SoundFlow  |
| Case 9  | Concrete 14 [cm] Single leaf structure BIS                  | SoundFlow  |
| Case 10 | Concrete 15 [cm] Single leaf structure BIS                  | SoundFlow  |
| Case 11 | Concrete 20 [cm] Single leaf structure BIS                  | SoundFlow  |
| Case 12 | Concrete 25 [cm] Single leaf structure BIS                  | SoundFlow  |
| Case 13 | Concrete 30 [cm] Single leaf structure BIS                  | SoundFlow  |
| Case 14 | Solid Brick 25 [cm] Double leaf structure ML                | dBKAisla   |
| Case 15 | Concrete 25 [cm] Double leaf structure CML                  | dBKAisla   |
| Case 16 | Concrete 15 [cm] 5x5x5 Double leaf structure BIS            | SoundFlow  |
| Case 17 | Concrete 15 [cm] 2.5x10x2.5 Double leaf structure BIS       | SoundFlow  |
| Case 18 | Concrete 15 [cm] 7x1x7 Double leaf structure BIS            | SoundFlow  |
| Case 19 | Concrete 25 [cm] 10x5x10 Double leaf structure BIS          | SoundFlow  |
| Case 20 | Concrete 25 [cm] 5x15x5 Double leaf structure BIS           | SoundFlow  |
| Case 21 | Concrete 25 [cm] 12x1x12 Double leaf structure BIS          | SoundFlow  |
| Case 22 | Concrete 30 [cm] 10x10x10 Double leaf structure BIS         | SoundFlow  |
| Case 23 | Concrete 30 [cm] 5x20x5 Double leaf structure BIS           | SoundFlow  |
| Case 24 | Concrete 30 [cm] 14x2x14 Double leaf structure BIS          | SoundFlow  |
| Case 25 | Brick Concrete 10 [cm] 5x5 Multilayer structure BIS         | SoundFlow  |
| Case 26 | Brick Concrete 20 [cm] 10x10 Multilayer structure BIS       | SoundFlow  |
| Case 27 | Brick Concrete 30 [cm] 15x15 Multilayer structure BIS       | SoundFlow  |



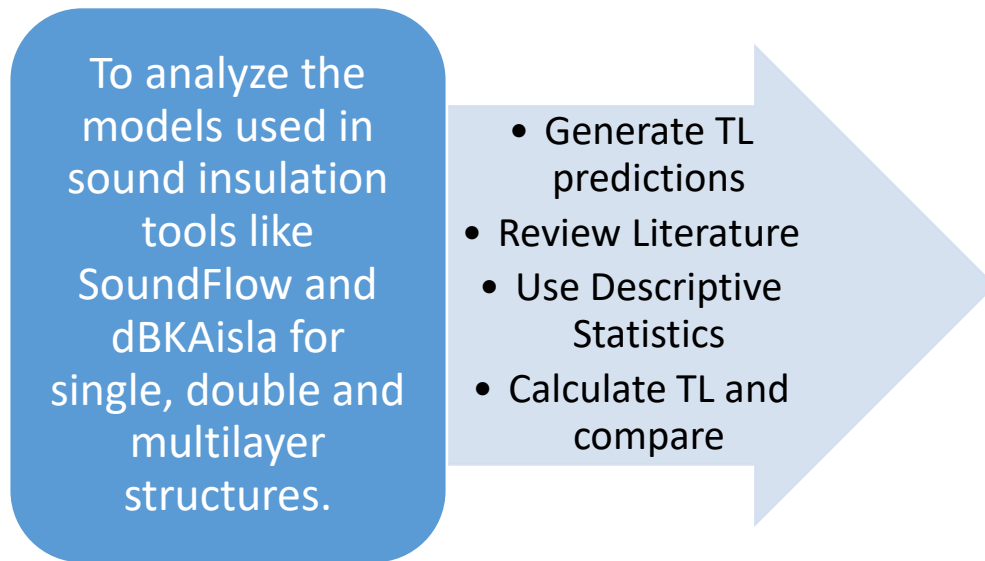


Figure 4 – Objective 1 “Definition”

Figure 4 visually summarizes what it means to accomplish the 1<sup>st</sup> specific objective of this thesis work and move on to the 2<sup>nd</sup> specific objective.

The number of materials that will be used for the cases in Table 7 is limited to two as explained in section 5.1.2 and the solid plate properties can be found in Table 6 of the same section.

#### **5.1.5 Steps to compare the prediction model used for multilayer components with Sharps method for multilayer elements.**

To measure the similarity or dissimilarity between two models, the first step is to present variables from the model for multilayer structures put forth by B.H.S Sharp (SHARP, 1969) and look at their counterparts in the model given by David A. Bies (A. Bies & H. Hansen, 2003). The second and final step involves a summary of the results found for each model. The solid plate properties for the materials used in the multilayer structure are presented in Table 6 section 5.1.2 Revising Literature.

#### **5.1.6 Process taken to evaluate the user interfaces for SoundFlow and dBKAisla**

To form an idea about the value and use of the SoundFlow and dBKAisla user interface, the first step will be to use both software to generate sound insulation predictions for single leaf, double leaf and multilayer structures. The second step will be to look at the delivery of the result sheets. The third and final step is, to compare the findings of the two previous steps. A visual representation to understand how to complete the 3<sup>rd</sup> specific objective is presented in Figure 5.

To form an idea of the value and use of the SoundFlow and dBKAisla user interface

- Generate TL predictions for SL, DL & ML.
- Generate Report sheets
- Display and compare findings of each software

*Figure 5 – Objective 3 “Definition”*

## Chapter VI: Results

Chapter VI gives tables and graphs that display all the information obtained in this thesis.

### 6.1 Software Selection.

#### 6.1.1 Software User Input and Result sheet

The parameters in Table 8 are all of those found in dBKAisla and SoundFlow, allowing a quick comparison between the different software when entering information to calculate TL predictions. The parameters associated with the solid plate properties in Table 8 are Young's modulus, Poisson's ratio, damping factor and density. The material database parameter refers to the software having its own database for materials used in typical constructions, materials such as concrete and brick.

Table 8 – Software Requirement Evaluation table

| dBKAisla | SoundFlow | Parameter                 |
|----------|-----------|---------------------------|
| ✓        | ✓         | Young's Modulus           |
|          | ✓         | Poisson's Ratio           |
| ✓        | ✓         | Plate Thickness           |
|          | ✓         | Plate dimensions          |
| ✓        | ✓         | TL model                  |
| ✓        | ✓         | Density                   |
| ✓        | ✓         | Damping factor            |
| ✓        | ✓         | User material input       |
| ✓        | ✓         | Material Database         |
| ✓        | ✓         | air cavity size           |
| ✓        | ✓         | Multiple Panel Definition |

Looking at the result sheets, we get different information from each software as seen in Table 9.

Table 9 – Results sheet comparison

| DBKAisla | SoundFlow | Results Sheet               |
|----------|-----------|-----------------------------|
| ✓        | ✓         | TL table                    |
| ✓        | ✓         | TL Graph                    |
| ✓        |           | ISO 717-1 Graph             |
| ✓        |           | Pink Noise R                |
| ✓        | ✓         | $R_w(C, C_{tr})$            |
| ✓        |           | Surface Density $M_s$       |
| ✓        |           | Coincidence Frequency $f_c$ |
| ✓        |           | Element Surface             |
| ✓        | ✓         | Damping factor              |
| ✓        | ✓         | Used material               |
|          | ✓         | TL model                    |
|          | ✓         | Direction of incidence      |
|          | ✓         | $C_{50-5000}$               |
|          | ✓         | $C_{tr50-5000}$             |
|          | ✓         | STC                         |
|          | ✓         | Plate dimensions            |
|          | ✓         | Plate thickness             |
|          | ✓         | Poisson's Ratio             |
|          | ✓         | Young's Modulus             |
|          | ✓         | Material Density            |

## 6.2 Single leaf, double leaf and multilayer structures

In this section, we will look at the results and set up the analysis of the different prediction models showcased in the theoretical framework. To automate the ISO 717-1 procedure a field measurement was carried out using the ISO 16283-1, as presented in the normative framework, obtaining data to work with and create an algorithm which interprets the data.

In section 6.2.1 Mass Law Single Leaf, a summary of the results of six cases using different prediction models referenced as the mass law will be shown. In section 6.2.2 SoundFlow Single Leaf, another seven cases will be summarized to study other prediction models for single leaf walls presented by the same authors mentioned in the theoretical framework. In section 6.2.3 SoundFlow Double Leaf, eleven cases dealing with double leaf structures are shown and the findings for each prediction model are presented. And in section 6.2.4 SoundFlow Multilayer

Structure, three cases will be presented to conclude results of different models used for airborne sound insulation or transmission loss values in the software SoundFlow and dBKAisla.

### 6.2.1 Mass Law Single Leaf

Refer to “Annex 1 Engineering Development” to look at the general results obtained for each case as well as the algorithms used.

Table 10 presents the range for the weighted sound reduction index  $R_w$ .

Table 10 – Broadband quantity analysis Cases 1-6

|              | Case 1<br>$R_w$ | Case 2<br>$R_w$ | Case 3<br>$R_w$ | Case 4<br>$R_w$ | Case 5<br>$R_w$ | Case 6<br>$R_w$ |
|--------------|-----------------|-----------------|-----------------|-----------------|-----------------|-----------------|
| Minimum      | 45              | 56              | 58              | 55              | 63              | 65              |
| Maximum      | 62              | 70              | 71              | 61              | 69              | 71              |
| Mean         | 57              | 65              | 66              | 58              | 66              | 68              |
| StnDeviation | 6               | 5               | 4               | 3               | 3               | 3               |
| CV           | 0.11            | 0.08            | 0.06            | 0.05            | 0.05            | 0.04            |

The models displayed in this section are presented in the theoretical framework as:

Equation [10] for David A. Bies, equation 34-37 for Randall F. Barron, equation [56] for Marshall Long and equation [77] for K.O. Ballagh. All of these representations for the mass law are valid to use and calculate transmission loss values.

In Table 11 we can see the variance for each independent prediction model, noticing that for almost all cases it has a value to which it tends to lean to.

Table 11 – Prediction models variance Cases 1-6

| Author    | Variance Case 1 | Variance Case 2 | Variance Case 3 | Variance Case 4 | Variance Case 5 | Variance Case 6 |
|-----------|-----------------|-----------------|-----------------|-----------------|-----------------|-----------------|
| dBKAisla  | 154             | 152             | 147             | 154             | 154             | 150             |
| Ballagh   | 154             | 154             | 154             | N/A             | 154             | 154             |
| Barron    | 154             | 154             | 154             | 154             | 161             | 154             |
| Long      | 154             | 154             | 154             | N/A             | 154             | 154             |
| Bies      | 154             | 154             | 154             | 154             | 154             | 154             |
| SoundFlow | 160             | 165             | 159             | N/A             | N/A             | N/A             |

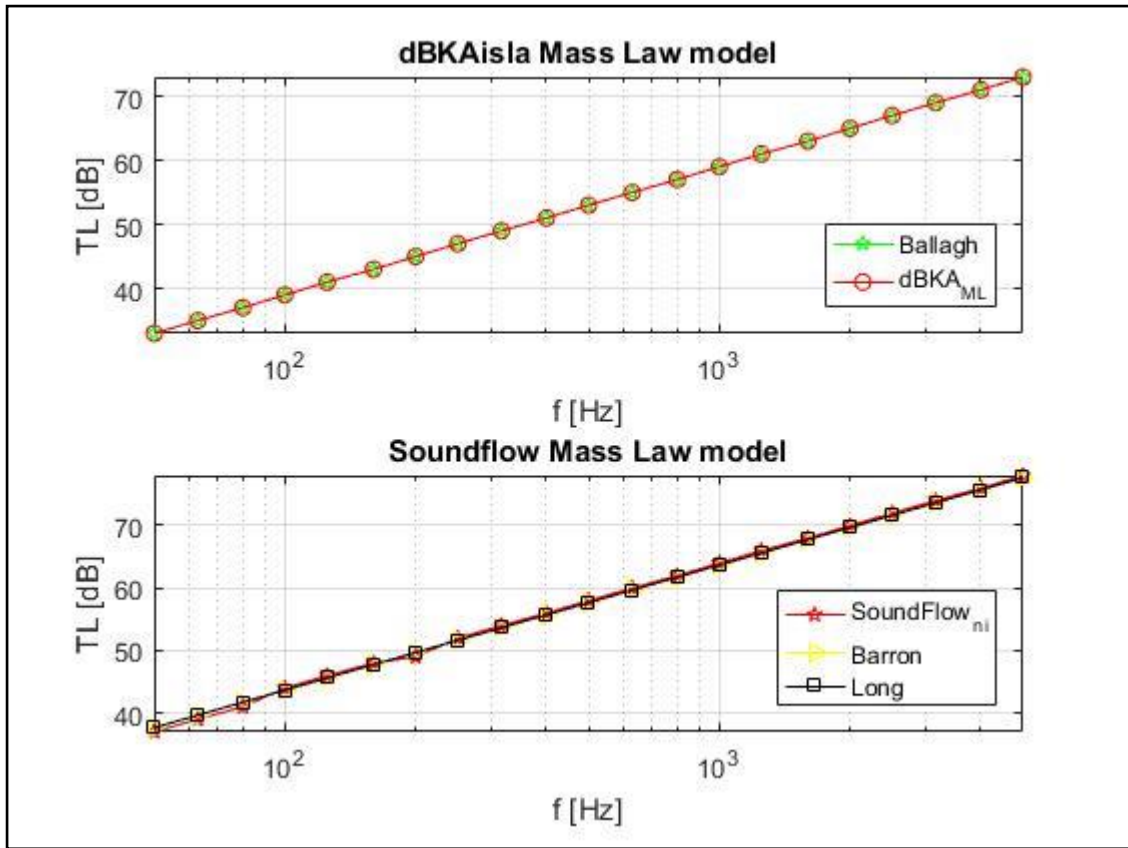


Figure 6 – Mass Law Model Case 1

### 6.2.2 SoundFlow Single Leaf

Refer to “Annex 1 Engineering Development” to look at the general results obtained for each case and its algorithms.

In Table 12 the range for the weighted sound indexes  $R_w$  is presented for cases 7-13.

Table 12 – Broadband quantity analysis Cases 7-13

|              | Case 7 | Case 8 | Case 9 | Case 10 | Case 11 | Case 12 | Case 13 |
|--------------|--------|--------|--------|---------|---------|---------|---------|
|              | $R_w$  | $R_w$  | $R_w$  | $R_w$   | $R_w$   | $R_w$   | $R_w$   |
| Minimum      | 34     | 41     | 46     | 45      | 45      | 52      | 53      |
| Maximum      | 45     | 49     | 59     | 59      | 62      | 58      | 60      |
| Mean         | 40     | 45     | 51     | 51      | 57      | 55      | 57      |
| StnDeviation | 4      | 3      | 5      | 5       | 6       | 2       | 2       |
| CV           | 0.10   | 0.07   | 0.10   | 0.10    | 0.11    | 0.04    | 0.04    |

The models analyzed in this section are presented in the theoretical framework as:

Section 2.1.3.2 Single Panel Transmission Loss for Marshall Long

Section 2.1.1.2 Panel Transmission Loss for David A. Bies

Section 2.1.2.3 A more intricate method that takes into account different variables as it builds the transmission loss curve. for Randall F. Barron.

Table 13 – Prediction models variance Cases 7-13

| Author        | Variance Case 7 | Variance Case 8 | Variance Case 9 | Variance Case 10 | Variance Case 11 | Variance Case 12 | Variance Case 13 |
|---------------|-----------------|-----------------|-----------------|------------------|------------------|------------------|------------------|
| SoundFlow     | 107             | 168             | 200             | 210              | 246              | 268              | 292              |
| Bies 1        | 125             | 172             | 206             | 207              | 237              | 262              | 286              |
| Bies 2        | 127             | 195             | 296             | 240              | 277              | 308              | 332              |
| Barron        | 113             | 175             | 206             | 233              | 265              | 311              | 346              |
| Long          | 174             | 272             | 310             | 362              | 395              | 449              | 445              |
| Thickness[cm] | 5               | 10              | 14              | 15               | 20               | 25               | 30               |

Figure 7 shows the different transmission loss curves calculated using the theories in the theoretical framework and compare it to the SoundFlow transmission loss curve.

Figure 8 shows the different transmission loss curves calculated using the theories in the theoretical framework as well but are shown to look at the low frequency deviations generated in the Randall F. Barron transmission loss model.

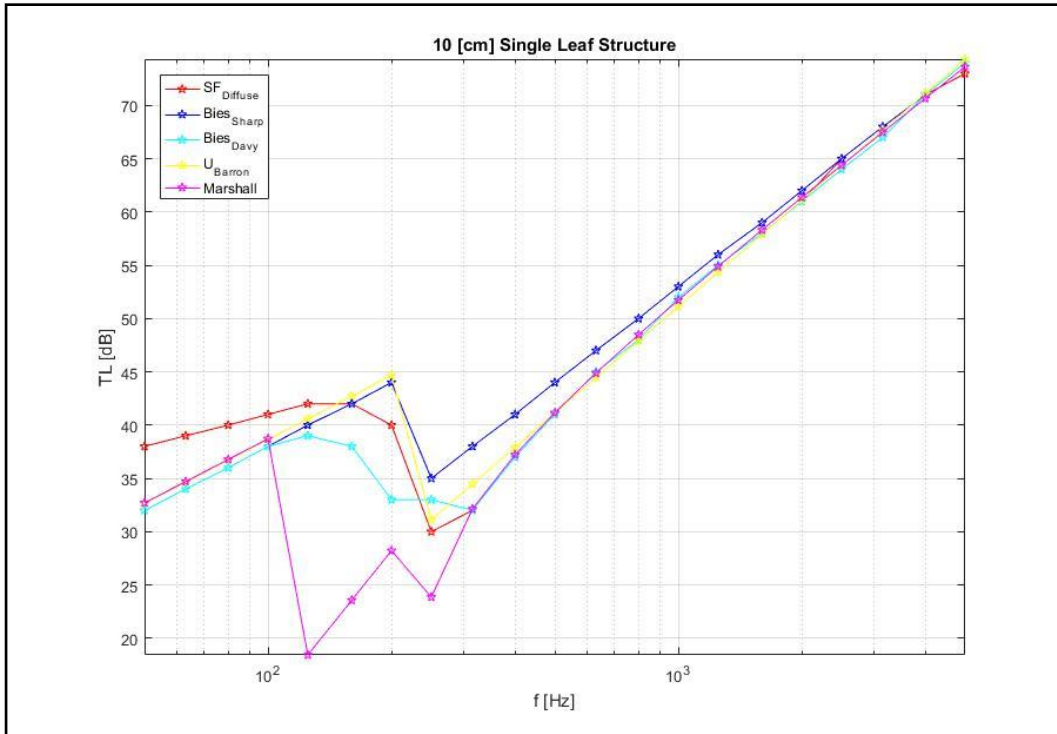


Figure 7 – David A. Bies 2<sup>nd</sup> model, Reference to Davy

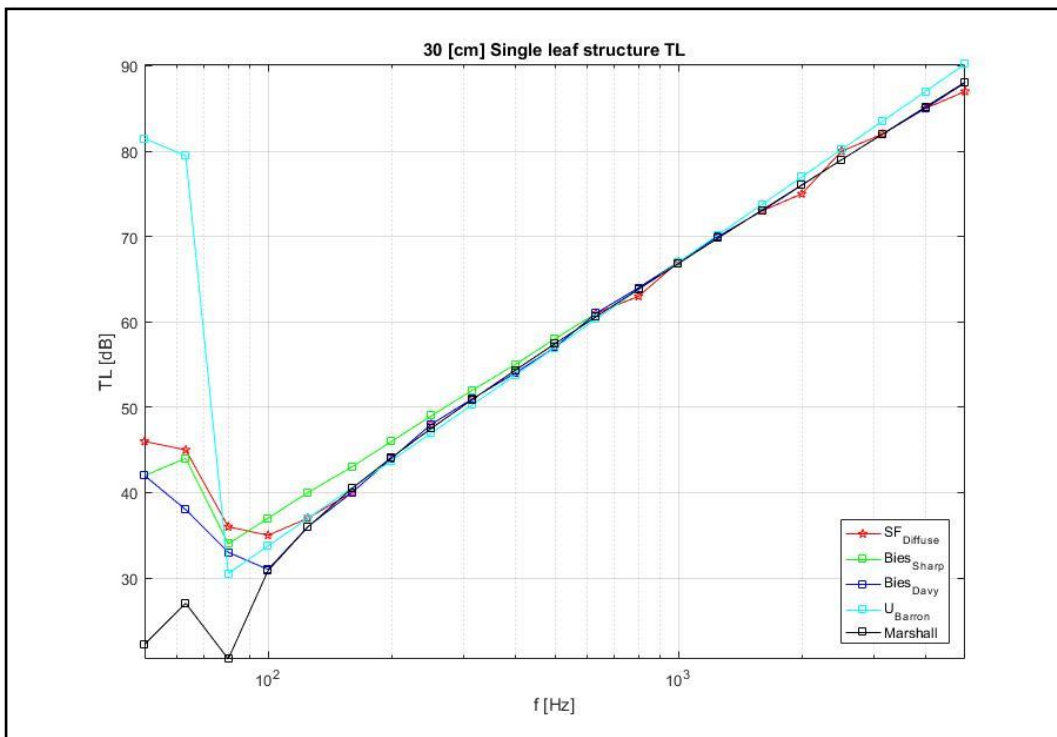


Figure 8 – Low frequency event Case 13



The different theories that were found in the data gathering process of this thesis work showed that for double leaf constructions, the models used to predict transmission loss for single leaf elements are used when constructing the prediction curve for the former. Considering this we move on to the double leaf type of construction.

### 6.2.3 SoundFlow Double Leaf

To look at the results displayed for the double leaf structures, the following four key points are essential.

First, in “Annex 1 Engineering Development” there will be a list of all cases and their general results. This section, covers cases fourteen to twenty-four.

Second, the double leaf partition will have a thickness  $h$  and three possible combinations to get that  $h$  value, as seen in the example shown in Table 14.

Table 14 – Example of possible combinations for thickness  $h$

| Combination          | Double Leaf Thickness [cm] |
|----------------------|----------------------------|
| 10[cm]x10[cm]x10[cm] | 30                         |
| 5[cm]x20[cm]x5[cm]   | 30                         |
| 14[cm]x2[cm]x14[cm]  | 30                         |

Third, the weighted sound reduction index will be analyzed using descriptive statistics on its transmission loss values as shown in Table 15.

Table 15 – Broadband quantity analysis Cases 14-24

| Case number   | Min [dB] | Mean [dB] | Standard Deviation [dB] | Max[dB] | CV   |
|---------------|----------|-----------|-------------------------|---------|------|
| Case 14 $R_w$ | 68       | 71        | 2                       | 74      | 0.03 |
| Case 15 $R_w$ | 68       | 73        | 5                       | 80      | 0.07 |
| Case 16 $R_w$ | 44       | 62        | 9                       | 69      | 0.15 |
| Case 17 $R_w$ | 40       | 59        | 11                      | 68      | 0.19 |
| Case 18 $R_w$ | 42       | 63        | 11                      | 71      | 0.17 |
| Case 19 $R_w$ | 52       | 69        | 9                       | 77      | 0.13 |
| Case 20 $R_w$ | 48       | 64        | 10                      | 77      | 0.16 |
| Case 21 $R_w$ | 49       | 68        | 10                      | 76      | 0.15 |
| Case 22 $R_w$ | 56       | 70        | 8                       | 80      | 0.11 |
| Case 23 $R_w$ | 49       | 65        | 10                      | 78      | 0.15 |
| Case 24 $R_w$ | 54       | 72        | 10                      | 79      | 0.14 |

Figure 9 presents the transmission loss curves for all the models used for a double leaf construction.

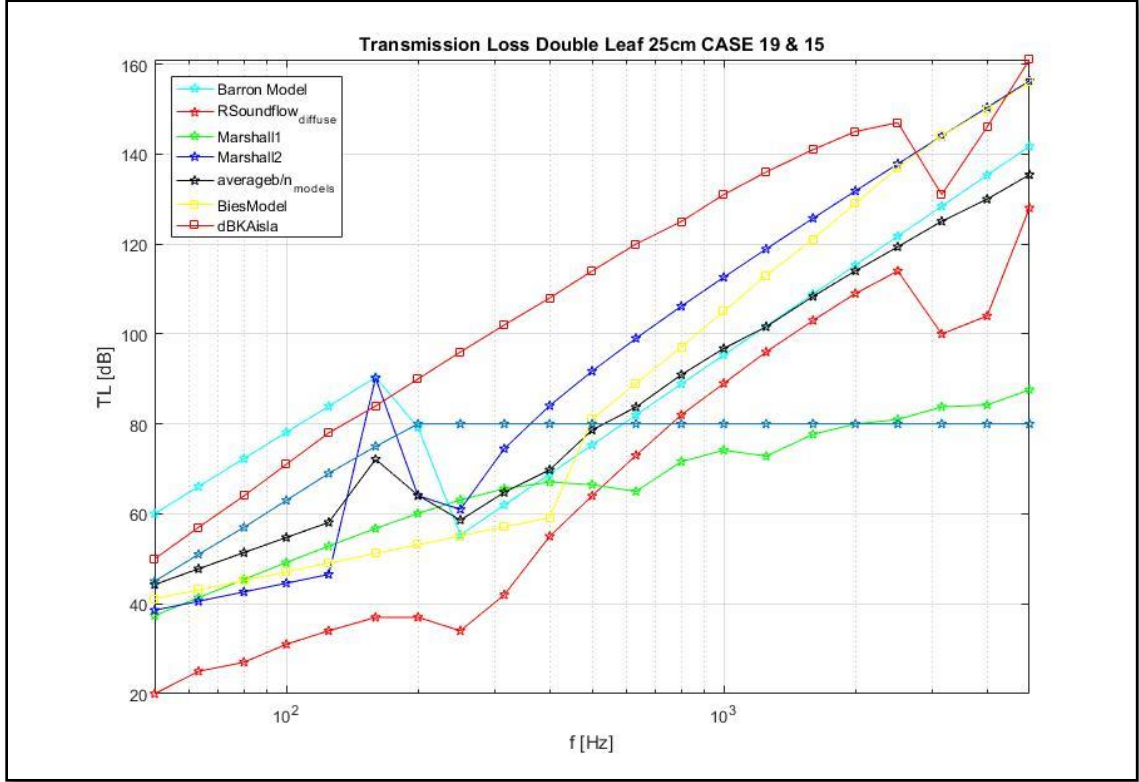


Figure 9 – Transmission loss predictions from all models

Fourth, there are three cases of study for the double leaf structures as seen in Table 16, Table 17 and Table 18.

Table 16 – Prediction models variance Cases 16-18

| Author         | Variance Case 16 | Variance Case 17 | Variance Case 18 |
|----------------|------------------|------------------|------------------|
| TLSF           | 944              | 522              | 1104             |
| TLBies         | 997              | 570              | 1224             |
| TLLong1        | 217              | 217              | 217              |
| TLLong2        | 1176             | 791              | 1369             |
| TLBarron       | 381              | 275              | 406              |
| TLAverage      | 581              | 391              | 655              |
| TLSFN          | 1139             | 894              | 1711             |
| Dimensions[cm] | 5x5x5            | 2.5x10x2.5       | 7x1x7            |

Table 17 – Prediction models variance Cases 19-21

| Author         | Variance Case 19 | Variance Case 20 | Variance Case 21 |
|----------------|------------------|------------------|------------------|
| TLSF           | 845              | 710              | 1396             |
| TLBies         | 1628             | 1051             | 1858             |
| TLLong1        | 217              | 217              | 213              |
| TLLong2        | 1529             | 1250             | 1653             |
| TLBarron       | 659              | 456              | 706              |
| TLAverage      | 845              | 639              | 905              |
| TLSFN          | 1088             | 723              | 1749             |
| Dimensions[cm] | 10x5x10          | 5x15x5           | 12x1x12          |

Table 18 – Prediction models variance Cases 22-24

| Author         | Variance Case 22 | Variance Case 23 | Variance Case 24 |
|----------------|------------------|------------------|------------------|
| TLSF           | 978              | 619              | 1540             |
| TLBies         | 1628             | 1051             | 2022             |
| TLLong1        | 217              | 217              | 217              |
| TLLong2        | 1529             | 1250             | 1551             |
| TLBarron       | 689              | 467              | 776              |
| TLAverage      | 863              | 645              | 942              |
| TLSFN          | 819              | 671              | 1427             |
| Dimensions[cm] | 10x10x10         | 5x20x5           | 14x2x14          |

Figure 10 presents a possible amalgamation between different models to stay within the established limits by SoundFlow.

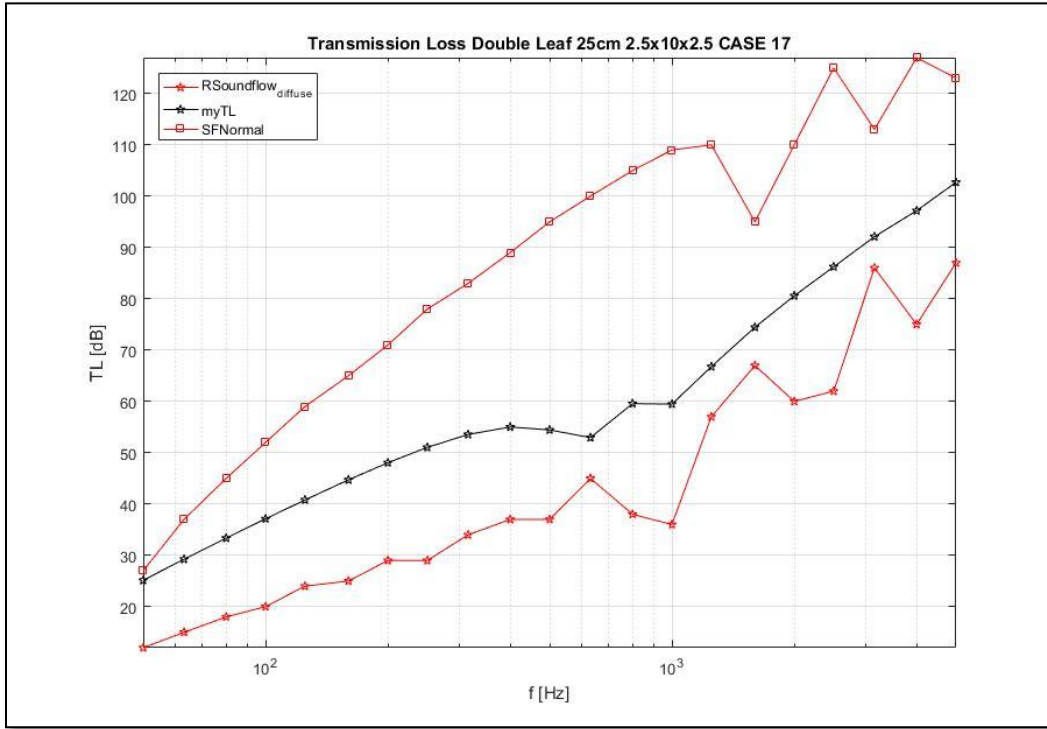


Figure 10 – Possible recommendation for transmission loss model

### 6.2.4 SoundFlow Multilayer Structure

Refer to “Annex 1 Engineering Development” to look at the general results obtained for the multilayer structures.

Introducing the definition of a multilayer element as any type of construction that has two or more layers, the cases are shown in Table 7 in section 5.1.4. The materials once again are brick and concrete and their solid plate properties can be found in Table 6 in section 5.1.2.

Table 19 – Broadband quantity analysis Cases 25-27

|               | Case 25 | Case 26 | Case 27 |
|---------------|---------|---------|---------|
| Mean          | 39      | 45      | 50      |
| Min           | 25      | 32      | 37      |
| Max           | 46      | 53      | 57      |
| Stn Deviation | 12      | 12      | 11      |
| CV            | 0.31    | 0.27    | 0.22    |

Table 20 – Prediction models variance Cases 25-27

| Author    | Variance Case 25 | Variance Case 26 | Variance Case 27 |
|-----------|------------------|------------------|------------------|
| Bies      | 182              | 257              | 313              |
| Barron    | 197              | 259              | 288              |
| SoundFlow | 92               | 149              | 188              |

Table 20 shows the variance that is measured when the models used are swapped while using the same critical frequency definition from Randall F. Barron. This option showed the best agreement with the predictions from SoundFlow when looking at both the weighted sound reduction index and the transmission loss values. As an opinion backed up by evidence, this occurs because of the definition used for the effective bending stiffness of the panel as defined by David A. Bies and the flexural rigidity as defined by Randall F. Barron as well as the distance to the neutral axis of the construction, depicted in section 2.1.1.4 and section 2.1.2.5 for both authors respectively.

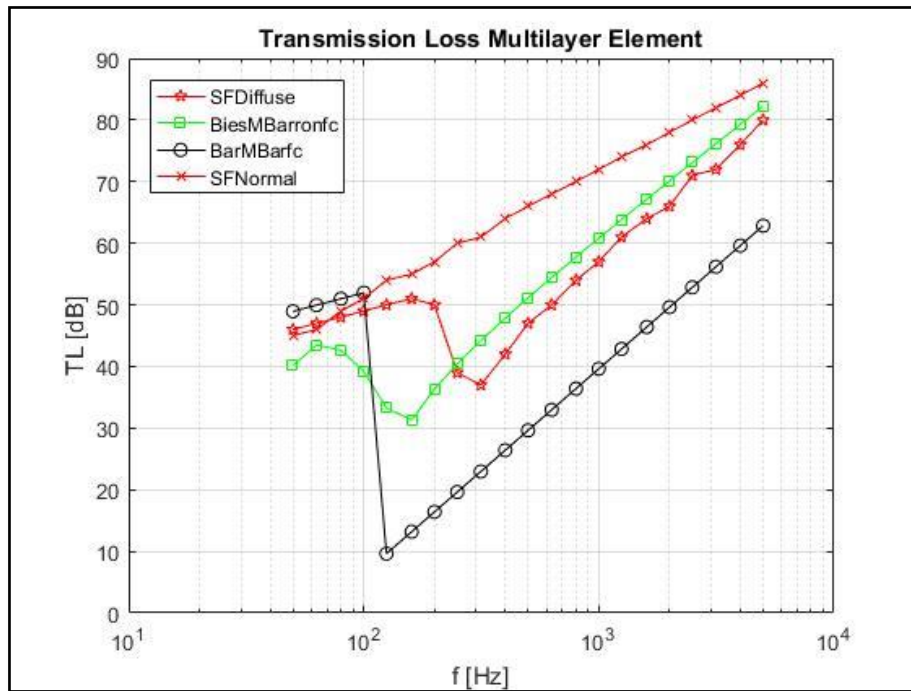


Figure 11 – TL multilayer element Case 26

In Figure 11, it can be seen that the Bies models creates a curve that is closer to the sound insulation prediction curve. Also, as shown in Figure 9, using the normal incidence prediction, one can establish an upper limit to the predictions. The definition given by Randall F. Barron for the damping coefficient is of vital importance because David A. Bies gives a more intricate definition that depends of different variables and is not as easy to set up. Also, it is not defined as a damping coefficient but as a panel loss factor, used in representing the damping controlled region of a panel.

## 6.3 Multilayer Model

### 6.3.1 Implementation of a specific algorithm

To implement the Sharp model, in the paper by B.H.S Sharp (SHARP, 1969), there is no direct reference to the use of a critical frequency. Instead, the author B.H.S Sharp mentions that the transmission coefficients  $R_i$  and  $T_i$  are obtained by means of the elastic constants represented as the bending and extensional impedances denoted by  $Z_B$  and  $Z_E$ . These definitions can be found in section 5.2.4.

The bending impedance can be looked at from its angle of incidence as well as its frequency. What can be observed is, that the imaginary part is represented in the figures as it varies in angle of incidence and frequency. In Figure 12 the imaginary bending impedance is depicted per frequency starting at 50 [Hz] and ending in 5000 [Hz].

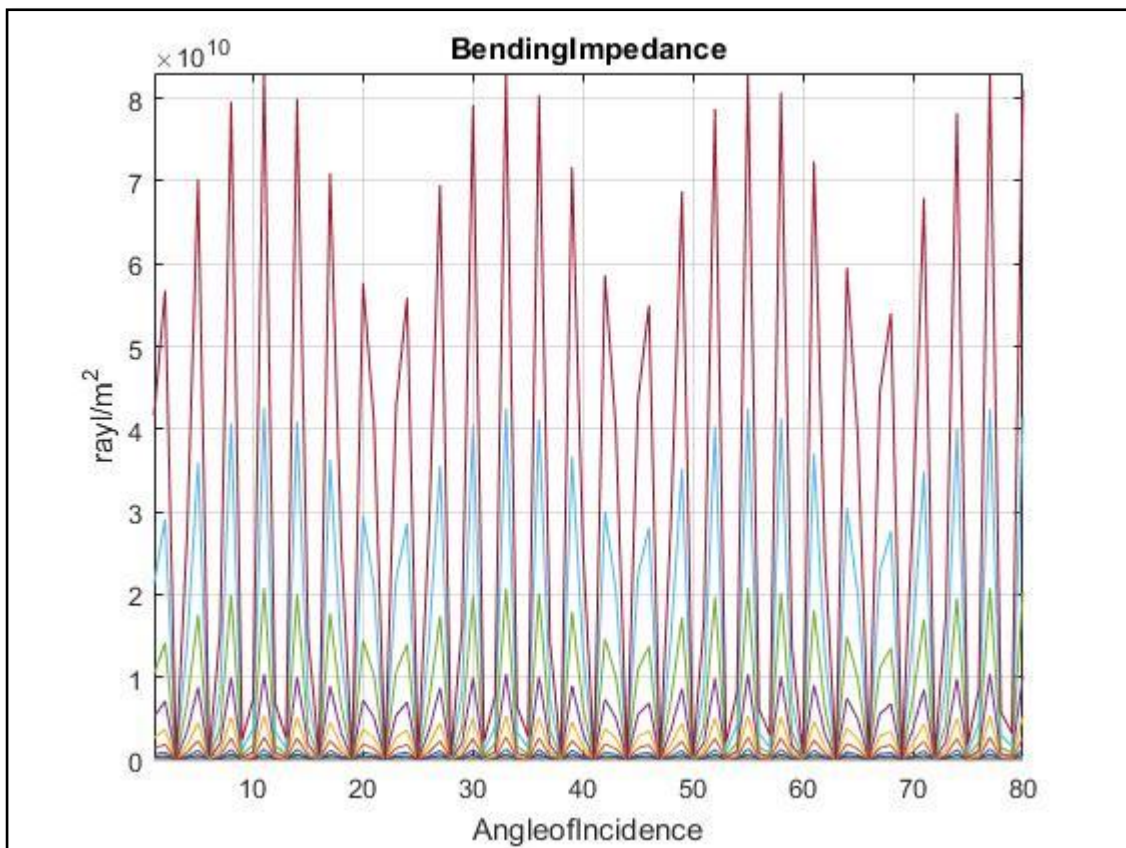


Figure 12 – Imaginary Bending Impedance vs Angle of Incidence (Res is 50 Hz, Blue is 63 Hz, Green is 80 Hz and it keeps increasing in one third octave bands)

In **Error! Reference source not found.** it can be seen how the angles of incidence generate bands per frequency because of the repetition seen in the different quadrants. The quadrants in this case would be quadrant I and quadrant II when looking at a Cartesian plane.

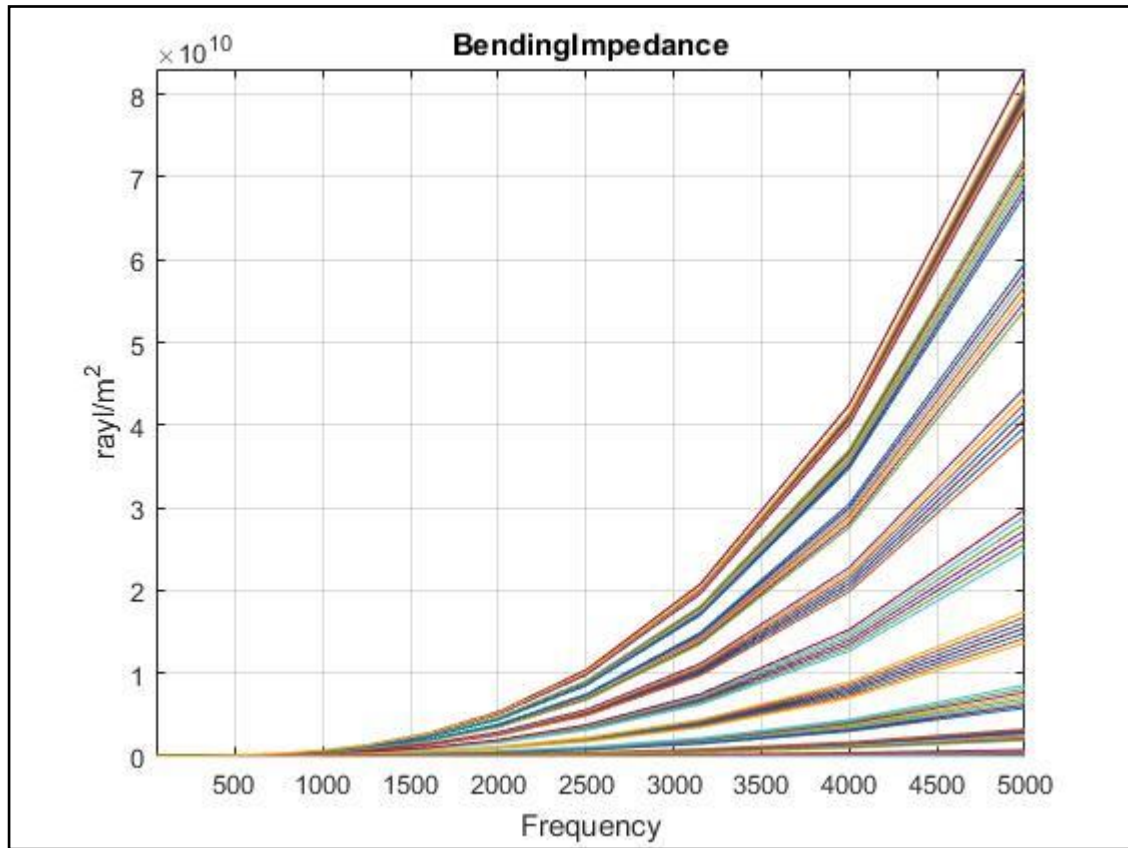


Figure 13 – Imaginary Bending Impedance vs Frequency (showing the frequency generated for different angles)

As seen with the bending impedance, the extensional impedance also presents values of 0 when its real part is looked at. The imaginary parts of the extensional impedance are presented in **Error! Reference source not found.** and **Error! Reference source not found.** where the latter shows the extensional impedance versus frequency and the former shows the extensional impedance versus angle of incidence.

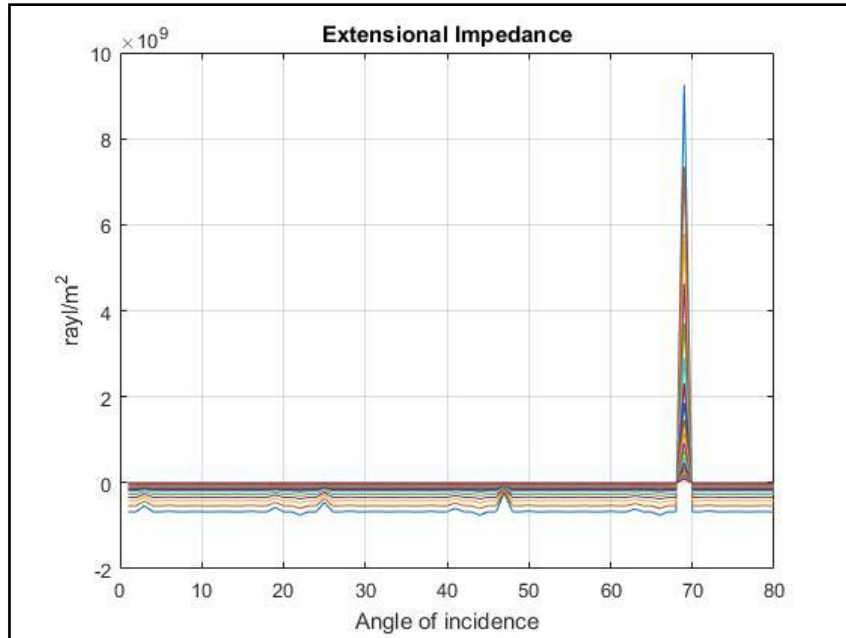


Figure 14 – Extensional Impedance vs Angle of Incidence (for different frequencies beginning in 50 Hz and moving in one third octaves to 5kHz)

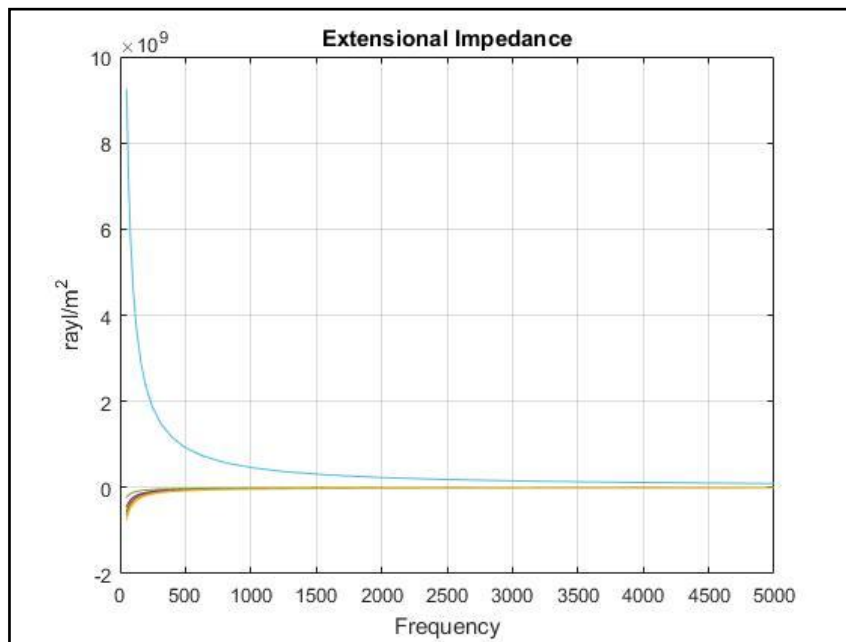


Figure 15 – Extensional Impedance vs Frequency (Blue is the Critical Frequency angles of incidence)

The author David A. Bies gives a definition for the bending impedance  $Z$  using a reference to Cremer. The same procedure is done to calculate this impedance values and



present them just as the bending and extensional impedance for sharp were presented. In Figure 16 we can see the bending impedance vs angle of incidence and notice that it has a similar result as that calculated for Sharps bending impedance definition when looking at it from its angle of incidence that was presented in Figure 12. In Figure 17 the same happens when the bending impedance definition from Bies-Cremer is calculated and presented with the x-axis as the frequency.

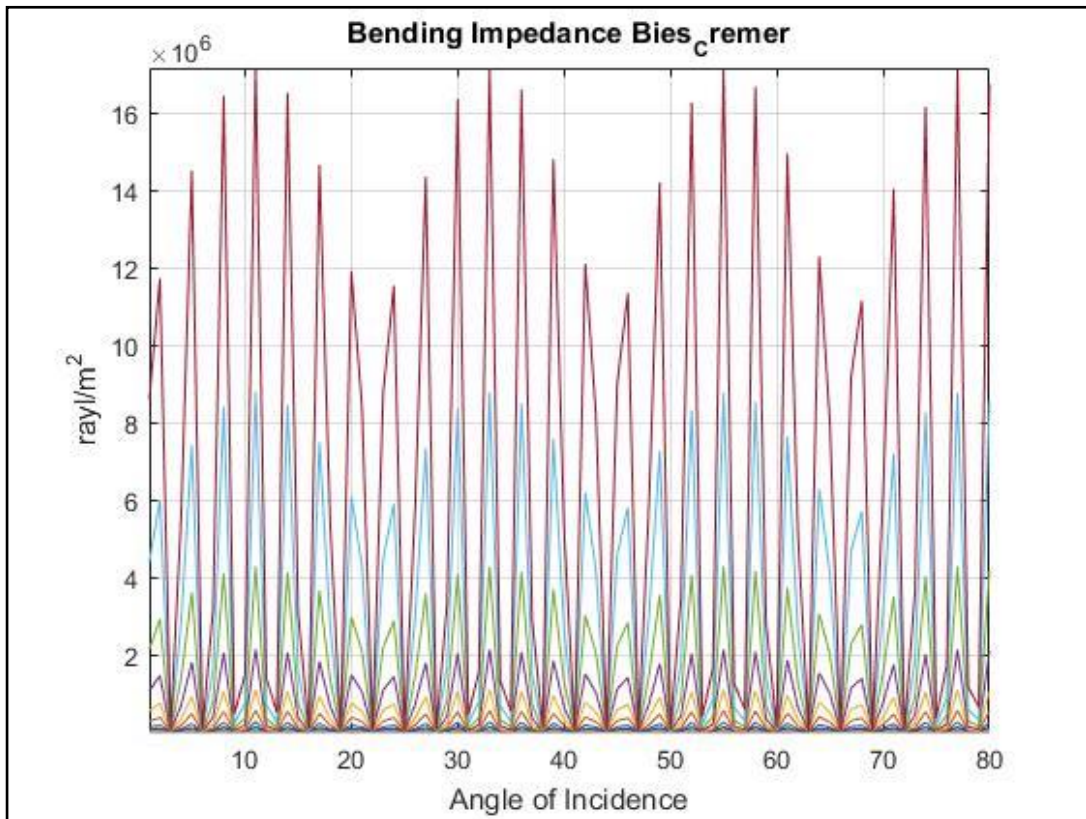


Figure 16 – Bending Impedance vs Angle of incidence Bies-Cremer (Red is 50 Hz, Blue is 63 Hz, Green is 80 Hz and it keeps increasing in one third octave bands until 5 kHz)

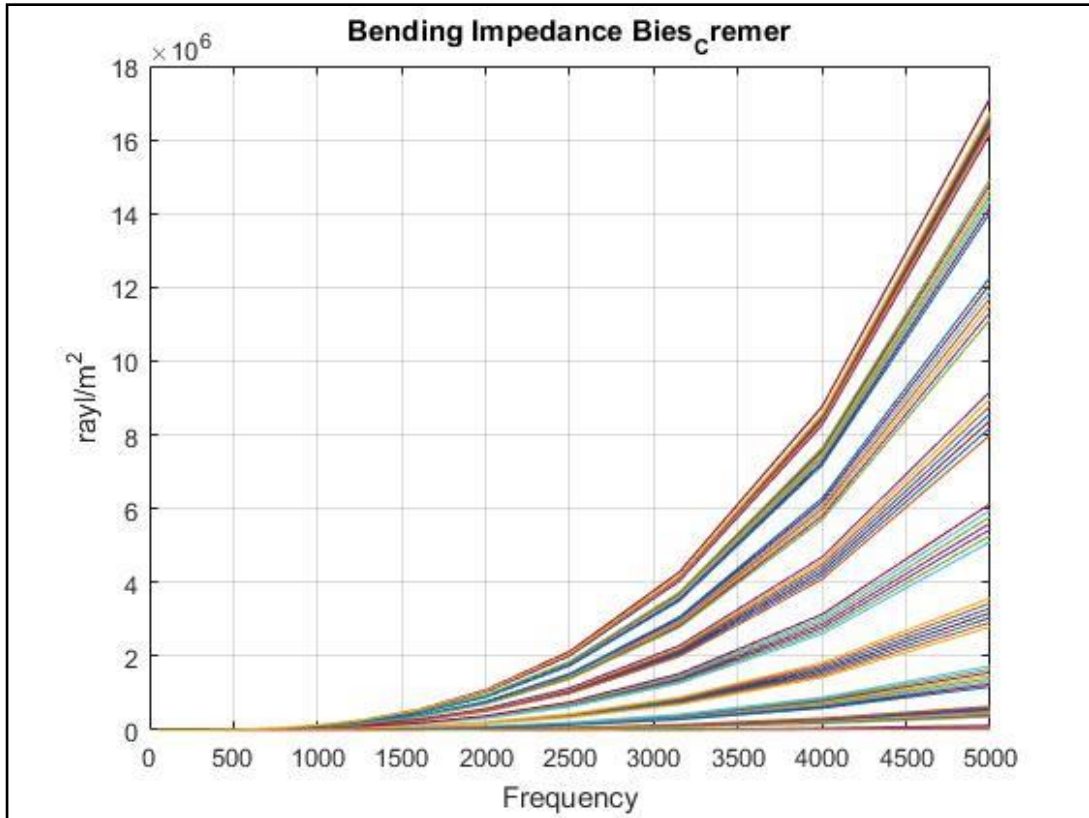


Figure 17 – Bending Impedance vs Frequency Bies-Cremer (Showing the frequency generated for different angles)

Continuing with the presentation of the different variables in the two models being compared, now comes the velocity of compressional waves from Sharp and the speed of propagation of bending waves from David A. Bies.

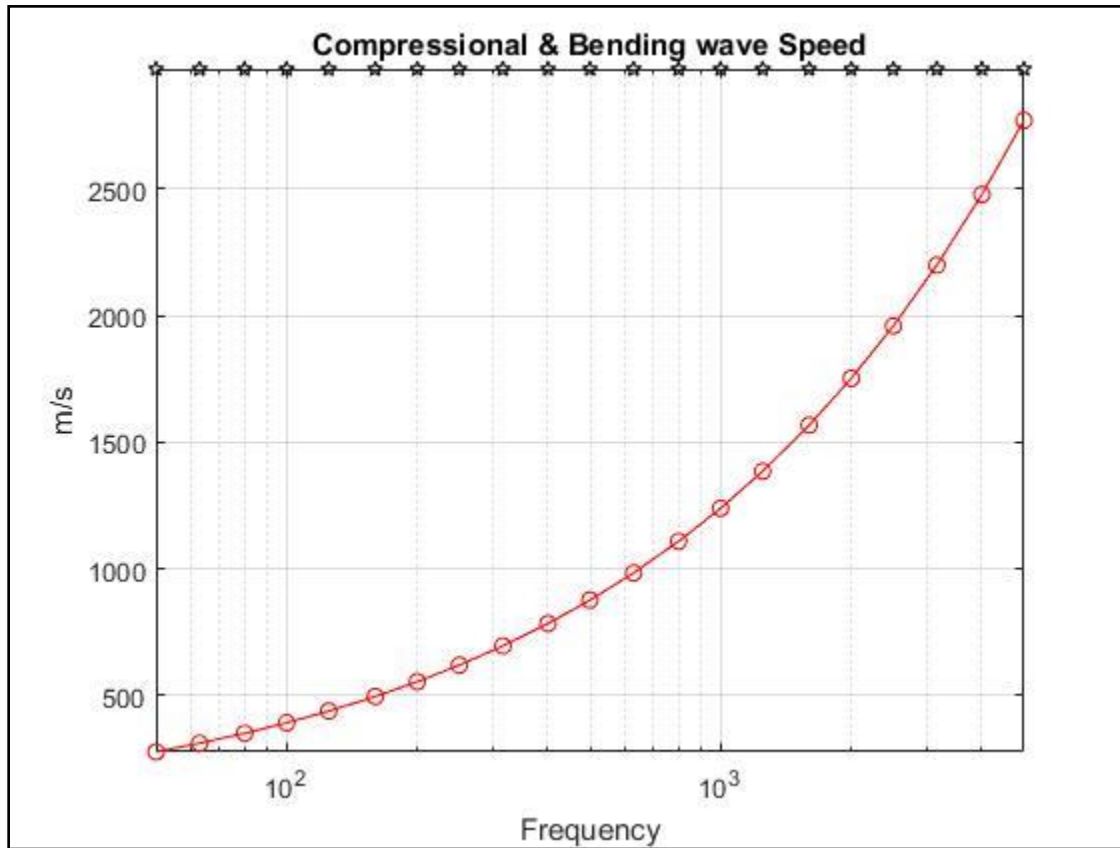


Figure 18 – Bending and compressional wave velocities (Red circles are Bies-Cremer and black stars are Sharp)

In Sharps model, the velocity of compressional waves alongside the velocity of shear waves is used to determine the extensional impedance and in turn determine an arbitrary constant that facilitates the calculation of the transmission and reflection coefficients  $T_i$  and  $R_i$ . On the other hand, the speed of propagation of bending waves is not used in the transmission loss model presented by David A. Bies.

#### 6.4 User Interface Evaluation

In this section, the step by step process of creating transmission loss predictions in software for such purposes will be presented, as well as some details of the results and report sheets. The first step by step process will be done for the dBKAisla software from Spain. The second step by step process will be done for the SoundFlow software from Germany. Afterwards a listing of some of their pros and cons will be detailed concluding the section. Refer to “Annex 1 Engineering Development” to look at the report sheets printed out by both software for different types of structures.

#### 6.4.1 dBKAisla

The first step to calculate sound insulation predictions with dBKAisla involves the choice of what type of model will be used. This software offers two choices to calculate its single leaf panel transmission loss. The first choice is the mass law and the second choice is the corrected mass law. By default, the program will select the corrected mass law model to predict the transmission loss curve but the mass law model will calculate the highest sound insulation values.

After choosing the prediction model that will be used, one needs to enter the data input. The software has its own data base with materials and their solid plate properties but it also allows the user to enter new materials and its solid plate properties. The information that the user will input for the material is the density, young's modulus, the damping loss factor and the thickness of the panel.

After the user enters the data, the software returns to the main interface showing the results from the users input on the left side of the screen, displaying the name, superficial mass or mass density, the critical frequency, the damping loss factor and the panel surface. These last three variables are not available when the user has chosen the mass law type of calculation.

After the user has entered the data and this data is reflected on the main screen, the program can now predict the transmission loss values for that type of structure using the selected type of calculation. The type of structure selected for this evaluation was the single leaf construction using concrete as its base material. The result sheet that the software delivers at the end when one chooses to create a report session, is delivered in a word format and gives the option of selecting what structure and calculation to put in the report if the working session has more than one construction at a time. For the double leaf type of construction, the user must choose what type of calculation will be used. It offers a vertical and horizontal type of calculation. After selecting the type of calculation whether it is a horizontal or vertical element, the user needs to define the layers that will be used and the distance between them. If the layer has not been created in the single leaf panel tab of the software than the layers cannot be defined in the double leaf panel tab of the software.

For this case being constructed with a single leaf structure using concrete and a double leaf structure using brick, the results in the report sheet will have an information segment which gives the client, address, material used for the structure and a comment area. For the transmission loss of the structure, it gives a graph of the values calculated superposed against the ISO 717-1 reference curve. It also give a table that shows the transmission loss calculated per one third octave bands. After the table and graph, it lists the weighted sound reduction index to pink noise, the weighted sound reduction index base on the ISO717-1, the superficial mass, the critical frequency, panel surface area and internal damping value. In "Annex 1 Engineering Development" there are multiple examples of different report sheets from dBKAisla.

### **6.4.2 SoundFlow**

The first step to calculate transmission loss predictions in SoundFlow is to define the solid plate material and thickness. SoundFlow also allows the user to define or enter its own solid plate properties by clicking on the structure and choosing the edit button. After defining the solid plate properties and thickness for the type of structure, for the second step, one chooses the absorber model which controls the equations that are used to calculate the transmission loss and defines the dimensions of the wall as infinite, standard measurement or user defined. Like dBKAisla, there are broadband quantities given for the transmission loss predictions.

SoundFlow allows the user to choose the direction of incidence from unidirectional, with an angle of incidence from 0 to 85 degrees and diffuse field with an average calculated over the mentioned angle range. The report sheet gives an image of the type of structure that is used and its material. After this, it gives the dimensions, type of backing of the structure and the absorber model that was used to calculate the transmission loss. It lists the solid plate properties used and broadband quantities. It gives information on the direction of incidence and the resolution of the data. In “Annex I Engineering Development”, an example of the report sheets printed by SoundFlow can be found.

### **6.4.3 Looking at some pros and cons**

The dBKAisla software has a module dedicated to the ISO 12354 which considers flanking transmission and can predict the sound insulation for a partition that is shared between two rooms as shown in the theoretical framework in Figure 2. This module can be seen in

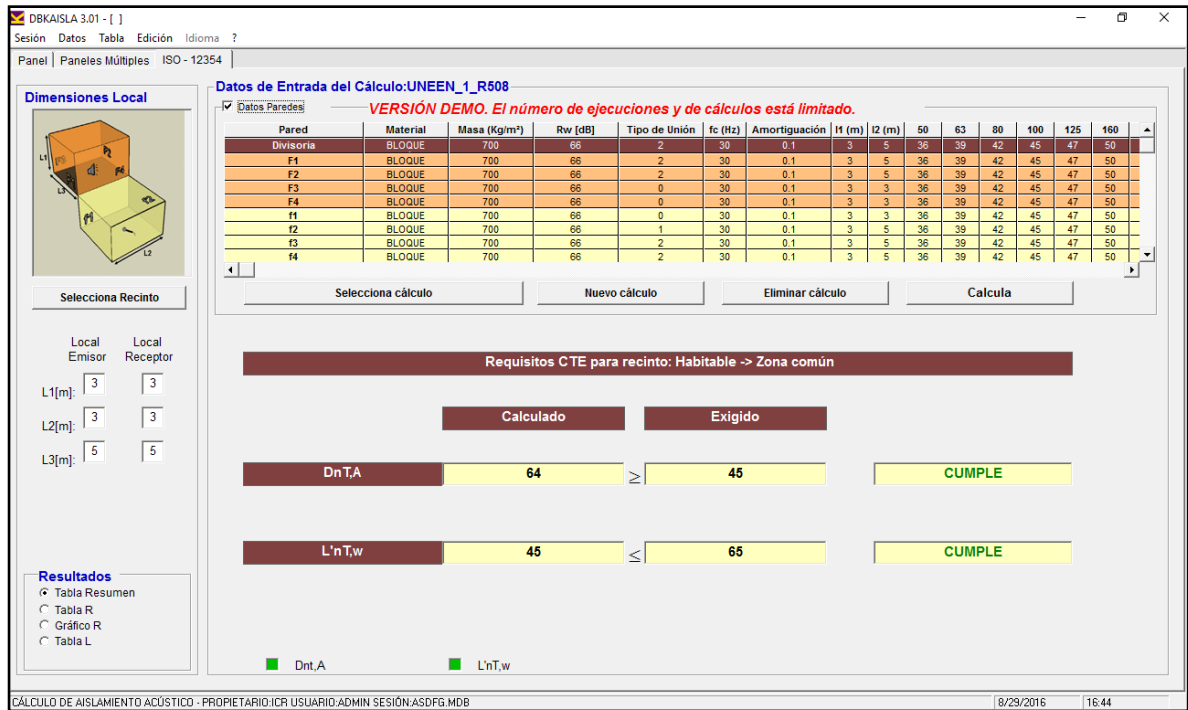


Figure 19 – dBKAisla ISO 12354 module

Looking at just the demo versions that were used, dBKAisla gives the user 15 sessions before blocking itself and leaving the user the only option of purchasing the software. For each session, in the single panel tab, it allows the user up to four predictions. In the multiple panels tab, it only allows the user one prediction before blocking itself. Comparing this with SoundFlow, it can be taken as a con because instead of fifteen sessions for a user, SoundFlow gives an individual a whole month to use the software and the predictions for single leaf or double leaf are not limited like in dBKAisla. Also, SoundFlow gives the user the option of changing the absorber model that will be used to calculate the transmission loss as well as the angle of incidence, dBKAisla does not give the latter and is restricted to only two models used in the calculation of transmission loss. In SoundFlow, the graphs of the transmission loss can be switched with tables reducing the amount of space that is used where as in dBKAisla, it presents the global values with the transmission loss calculated for the construction element and is not placed on its own segment displaying only broadband quantities like SoundFlow.

## 6.5 Transmission loss and the weighted sound reduction index

In both software, the double leaf structures use the transmission loss values that were calculated for the single leaf layers to build the double leaf structure transmission loss. They also use a damping loss coefficient variable defined by the solid plate properties of the layers in a multilayer structure to generate transmission loss values using the single leaf prediction model. The column highlighted entirely in yellow is the reference value for each table. The values from other models that are highlighted in yellow depict the exact target value while the ones in green

show the nearest value. The purpose of this is, to find the weighted sound reduction index that is closest to the reference model.

Table 21 – Cases 1-6 analysis

| Case number | SFR <sub>w</sub> | dBKAR <sub>wCML</sub> | dBKAR <sub>wML</sub> | Barron | Bies1 | Ballagh | Long |
|-------------|------------------|-----------------------|----------------------|--------|-------|---------|------|
| 1           | 45               | 46                    | 57                   | 62     | 57    | 57      | 62   |
| 2           | 56               | 54                    | 65                   | 70     | 65    | 65      | 70   |
| 3           | 58               | 56                    | 67                   | 71     | 66    | 67      | 66   |
| 4           | 45               | 45                    | 56                   | 61     | 55    | NA      | 61   |
| 5           | 54               | 53                    | 64                   | 69     | 63    | 64      | 69   |
| 6           | 56               | 56                    | 67                   | 71     | 65    | 66      | 71   |

It is important to keep in mind that Bies 1 refers to the David A. Bies model referenced to Sharp while Bies 2 refers to the David A. Bies model reference to Davy.

Table 22 – Cases 7-13 analysis

| Case number | SFR <sub>w</sub> | dBKAR <sub>wCML</sub> | dBKAR <sub>wML</sub> | Barron | Bies1 | Bies2 | Long |
|-------------|------------------|-----------------------|----------------------|--------|-------|-------|------|
| 7           | 39               | 41                    | 51                   | 42     | 45    | 41    | 34   |
| 8           | 45               | 46                    | 57                   | 46     | 49    | 46    | 41   |
| 9           | 49               | NA                    | NA                   | 50     | 52    | 49    | 46   |
| 10          | 49               | 49                    | 61                   | 50     | 52    | 50    | 45   |
| 11          | 53               | 52                    | 63                   | 53     | 56    | 53    | 50   |
| 12          | 56               | 54                    | 65                   | 55     | 58    | 56    | 52   |
| 13          | 58               | 56                    | 67                   | 57     | 60    | 57    | 55   |

Table 23 – Cases 16-24 Analysis

| Case number | SFR <sub>w</sub> | Barron | Long1 | Long2 | Bies |
|-------------|------------------|--------|-------|-------|------|
| 16          | 44               | 69     | 64    | 60    | 67   |
| 17          | 40               | 68     | 58    | 54    | 67   |
| 18          | 42               | 66     | 67    | 65    | 68   |
| 19          | 52               | 77     | 70    | 71    | 68   |
| 20          | 48               | 77     | 64    | 61    | 67   |
| 21          | 49               | 71     | 72    | 72    | 68   |
| 22          | 56               | 80     | 70    | 71    | 68   |
| 23          | 49               | 78     | 64    | 61    | 67   |
| 24          | 54               | 79     | 73    | 77    | 68   |

Table 24 – Cases 25-27 Analysis

| Case number | SFR <sub>w</sub> | Barron | Bies |
|-------------|------------------|--------|------|
| 25          | 46               | 25     | 45   |
| 26          | 51               | 32     | 53   |
| 27          | 55               | 37     | 57   |

## 6.6 ISO 717-1

To look at the weighted sound reduction index from each prediction model and its difference from the chosen software reference that was analyzed, in the section titled “ISO 717-1 Automated process check” found in “Annex 1 Engineering Development” there is a table titled “Sound Reduction Index ISO 717-1 Automated Check” that is used to determine if the automated process developed for the ISO 717-1 is acceptable. The results from this are displayed ahead.

For cases 1-6 the analysis carried out in SPSS, Statistical Package for the Social Sciences, is shown in Figure 20. In this figure, we can see that the automated process developed for the ISO 717-1 gives sound reduction index values that are closest to its intended reference, in this case, the dBKAisla software values. The transmission loss values used for SoundFlow were those calculated using normal incidence, the transmission loss values for dBKAisla were those from the mass law model. Looking at both curves, the lowest sound reduction index is given in SoundFlow while dBKAisla presents the upper limit as seen in Figure 20.



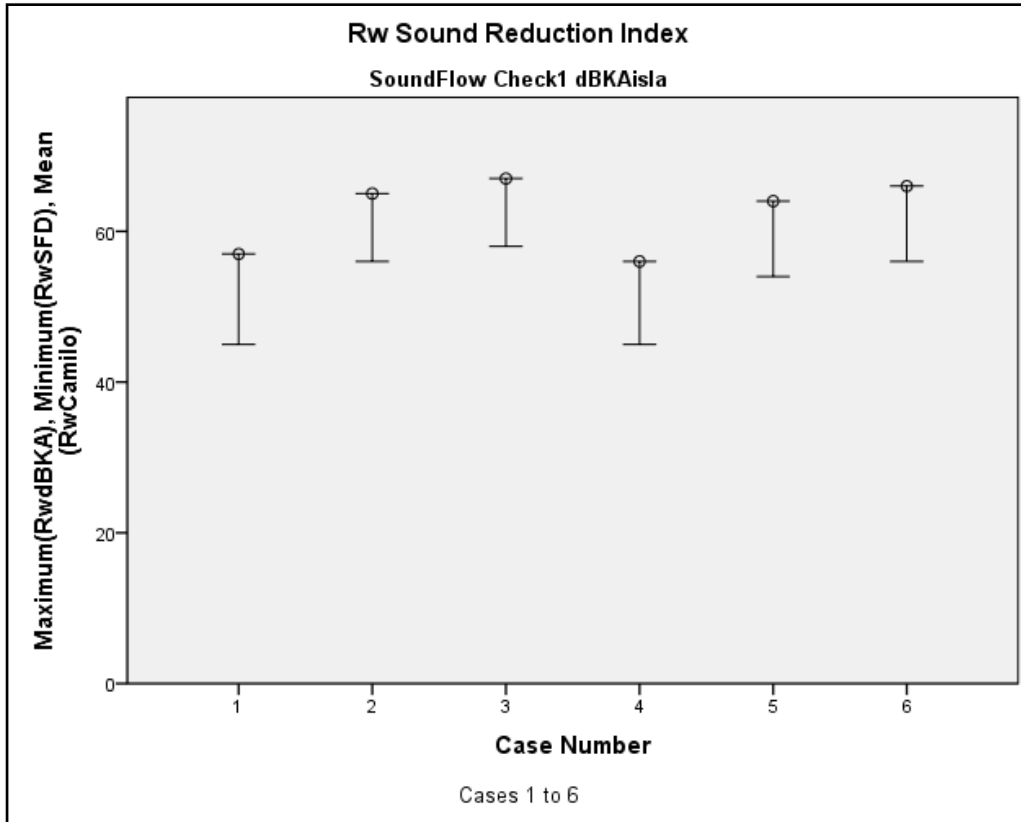


Figure 20 – SPSS Analysis Cases 1-6

For cases 7-13 the analysis done in SPSS is shown in Figure 21. Here the reference model is SoundFlow and again, the calculated values are very close to those presented by the reference. This time the transmission loss analyzed, is that of the diffuse field option given by SoundFlow and establishes the lower limit. The upper limit is given by the application of the ISO 717-1 automated process to the normal incidence transmission loss generated by SoundFlow and the nearest value to the reference in each case is given by the application of the same ISO 717-1 automated process to the diffuse field transmission loss data predicted by SoundFlow.

Cases 14 and 15 were skipped because of lack of a lower limit, this happened because of the limitation given by the dBKAisla demo in only allowing the user 15 sessions to work with. Skipping those two cases, the next analysis will be presented for cases 16-24.

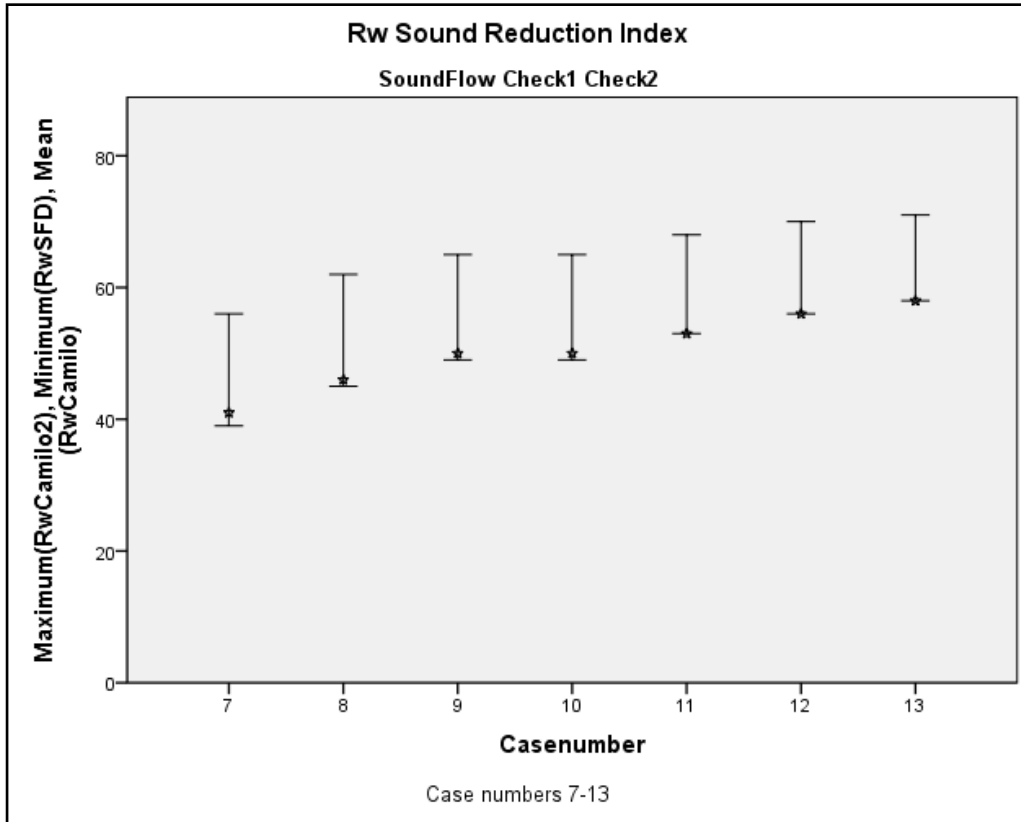


Figure 21 – SPSS Analysis Cases 7-13

For cases 16-24, the analysis in SPSS shows, again, that the application of the ISO 717-1 automated process in the diffuse field transmission loss values give a closer sound reduction index to those generated by SoundFlow in each case. This can be seen in Figure 22.

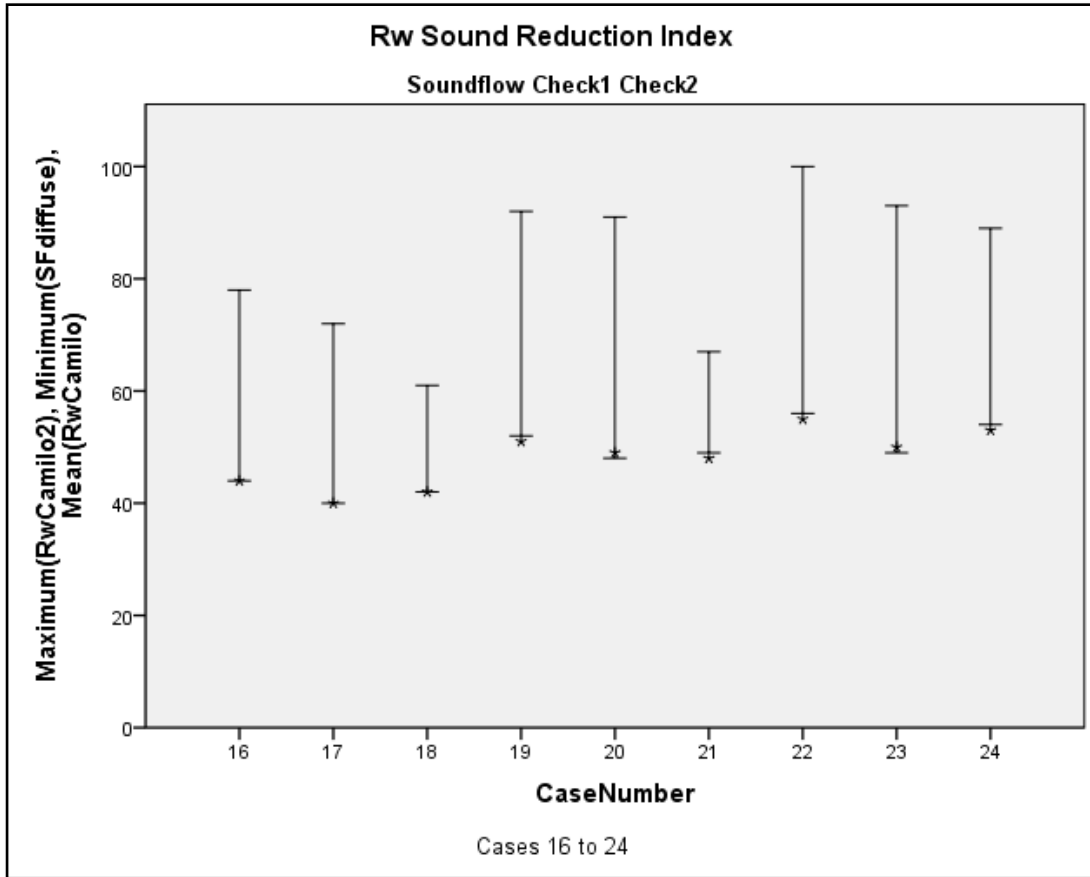


Figure 22 – SPSS Analysis Cases 16-24

For the final cases, cases 25-27, the same procedure is done in SPSS. Again, the results show that the sound reduction index calculated by the ISO 717-1 automated process is closer when the diffuse field transmission loss values generated in SoundFlow are used instead of the normal incidence transmission loss. The upper limit is always given by the application of the ISO 717-1 automated process to the normal incidence transmission loss values generated by SoundFlow. This can be seen in Figure 23.

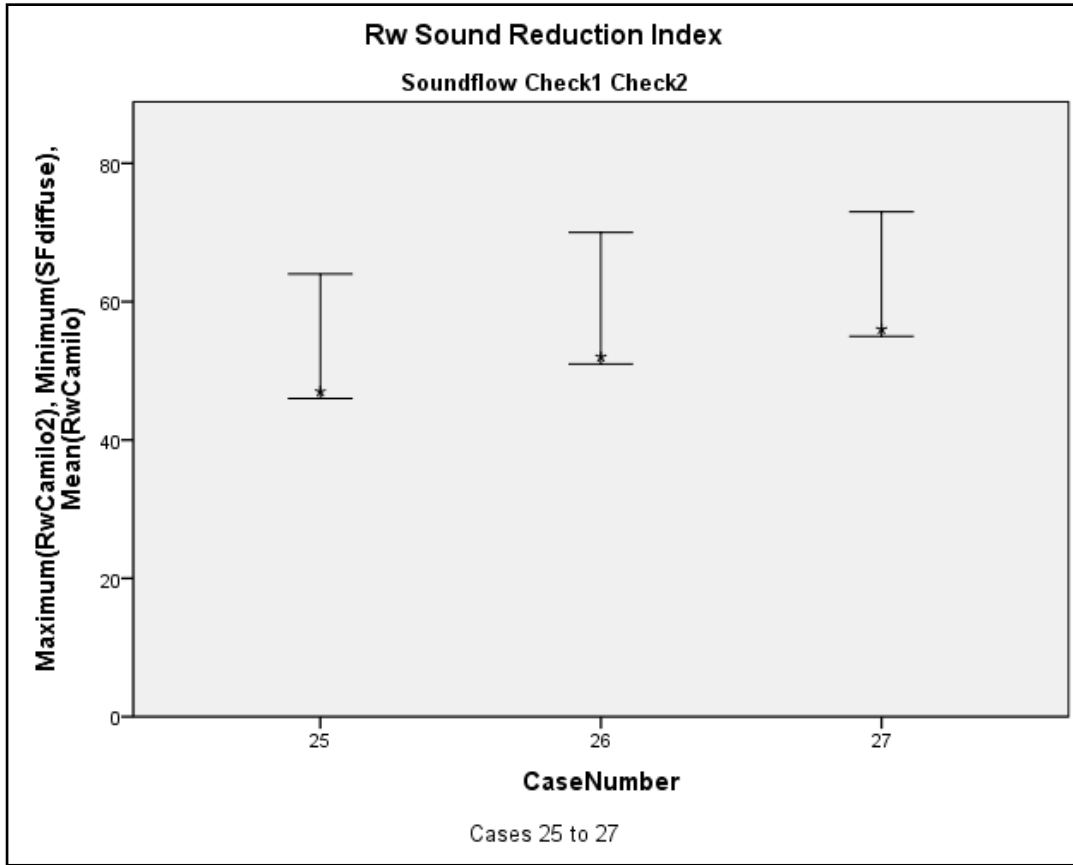


Figure 23 – SPSS Analysis Cases 25.-27

## **Chapter VII: Discussion**

### **7.1 Software Selection**

Looking at Table 8, the lack of the parameter Poisson's ratio in dBKAisla wouldn't seem to create such large variations since it usually takes a value between 0 and 1. This in the transmission loss is reflected as a relatively small fluctuation in the transmission loss values. And to this, it can be ignored.

From Table 9 it can be inferred that each software and company deliver different results according to their own needs. Looking at the common ground we find that both make use of tables and graphs to display the transmission loss curve. While the weighted sound reduction index is given in both, dBKAisla and SoundFlow, it can be seen in Table 9 that SoundFlow gives the default and extended range weighted sound reduction index. To end the common ground, the damping factor and the material used are given in both result sheets.

### **7.2 Single Leaf, Double Leaf and Multilayer Structures**

#### **7.2.1 Mass Law Single Leaf**

As can be seen with its standard deviation in Table 10, the data seems to present a normal distribution for the first six cases as obtained by the mass law theory and the predictions from SoundFlow and dBKAisla. The models used from Randall F. Barron, Marshall Long and David A. Bies tend to agree with SoundFlow as opposed to the Ballagh prediction model which tends to agree with dBKAisla, as can be seen in Figure 6.

#### **7.2.2 SoundFlow Single Leaf**

Again in Table 12 it can be noted that the standard deviation for all cases is relatively small considering none has reached a two-digit value. In Table 13 we can see that the variance for each model has a different value as opposed to cases 1-6 where they all tended to one particular value. From this, in turn, we can assume that the data for the transmission loss predictions is no longer inclining to a normal distribution type of data, where as its weighted sound reduction index values are relatively close to each other. It can also be noted that as the thickness of the single leaf construction increases so does the variance for each transmission loss model, where as in cases 1-6 they remained around the same value regardless of the thickness of the construction.

In Figure 7, around the range of the critical frequency, the 2<sup>nd</sup> prediction model by author David A. Bies referenced to Davy tends to try to take the shape of the SoundFlow transmission loss prediction. As opposed to the prediction models presented by Randall F. Barron, Marshall Long and the 1<sup>st</sup> model proposed by David A. Bies referenced to Sharp.

It is also important to note that for low frequency in panels that start to exceed 25[cm], the Randall F. Barron transmission loss model begins to generate values that are several times greater than the other models. In this range the best predictions tend to lie with the David A. Bies models as can be seen in Figure 8.

Figure 7 and Figure 8 can also be used to show that all the transmission loss curves calculated above the critical frequency have lower discrepancies when compared to the values below said frequency.

### **7.2.3 SoundFlow Double Leaf**

Comparing the standard deviation from Table 10 and Table 12 to Table 15, we can see that the central tendency occurs only in the dBKAisla model because of its upper limit value being set as 80 [dB], as seen in Figure 9 . For this reason, the software of interest to analyze in double leaf structures now becomes SoundFlow.

From Figure 9 we can also look at the two predictions used by SoundFlow to create a range of where the transmission loss curve should be. The highest value for the SoundFlow predictions is calculated in normal incidence while the lowest values are calculated in diffuse field.

Table 16, Table 17 and Table 18, show that the lowest variance in the data for the different combinations used for double leaf structures occurs when the air gap is larger than its layers. For this specific combination, the mix between the model by Marshall Long presented in section 2.1.3.3 Double Leaf Transmission Loss is used for whenever any given frequency is below the critical frequency and the model presented by Randall F. Barron in section 2.1.2.4 Composite Wall with an Airspace Transmission Loss is used for any frequency above the critical frequency. This combination of transmission loss models allows the calculation of transmission loss values that are within the established range by the normal incidence prediction and diffuse field predictions. Figure 10 shows case seventeen and the transmission loss predictions based on the possible amalgamation recommended above.

To clarify the three cases that are being studied, the first case is when the layers are equal in size to the air gap or cavity of the double leaf construction or similar in size. The second case, takes place when the air gap or air cavity is larger than the composing layers of the double leaf construction. The third and final case of study occurs when the layers are larger than the cavity. Again, as can be seen in Table 16, Table 17 and Table 18. In Figure 10 the myTL curve represents the results for the amalgamation between Marshall Long and Randall F. Barron that was proposed earlier.

### **7.2.4 SoundFlow Multilayer Structure**

Looking at Table 19, one can see that the standard deviation in this structure tends to have a higher value when compared to those in Table 10 and Table 12 from the single leaf transmission loss predictions.

## **7.3 Multilayer Sharp**

The variables that describe the solid plate properties of a material, are used to obtain the compressional and shear wave velocities. These are given in equation [99] and equation [100]. This constant velocity is used to find the bending and extensional impedance of a panel and by doing so, it allows the user to obtain the arbitrary constant C, as seen in “Annex 1 Engineering

Development”, which is of vital importance to determine the transmission and reflection coefficients.

One of the main differences that can be seen from Sharps model and David A. Bies model is the behavior seen in for the compressional and bending wave velocities as one of them is constant throughout the frequency range while the other varies accordingly, increasing as the frequency itself increases as seen in Figure 18.

#### **7.4 Transmission loss and the weighted sound reduction index**

In Table 21 the Barron transmission loss model is one of the models that is furthest away from the reference value given by dBKAisla. Also Table 21 shows that the models with the closest transmission loss are Bies and Ballagh.

In Table 22 it can be seen that the David A. Bies model referenced to Sharp and the transmission loss model by Marshall Long are the ones furthest away. The model presented by David A. Bies reference to Davy predicts the nearest weighted sound reduction index value when its target value is that given by SoundFlow. The second transmission loss model to achieve weighted sound reduction indexes near the target value is the Randall F. Barron transmission loss model.

In Table 23 which deals with double leaf transmission loss, the furthest transmission loss values calculated are those given by Randall F. Barron while the other models vary when generating the weighted sound reduction index values near the target value given by SoundFlow.

The final cases dealing with a multilayer element of two layers, presented in Table 24 show that the Bies model used, generates the weighted sound reduction index closer to that of the target value given by SoundFlow.

#### **7.5 ISO 717-1**

Looking at Figure 20, Figure 21, Figure 22 and Figure 23 it can become clear why the information from the field measurement using the ISO 16283 is omitted. The implementation of the normative was intended to generate vectors or arrays that had the same dimensions and data density to those obtained in a field measurement. To this end, it is not the data that is important but the amount of data and its way of being organized what matters.

## 7.6 Conclusions

1. From the different examples that were carried out, it can be inferred that SoundFlow always uses the diffuse field transmission loss prediction to calculate the weighted sound reduction index, as can be seen in section 5.7.
2. dBKAisla has a limiting value for transmission loss predictions at 80 [dB]. This changes the sound reduction index because it is not accounting for any value above this limit and starts to generate a data type with a central tendency and normal distribution. This can be seen in Figure 9 section 5.3.3.
3. For multilayer element constructions, thin structures are best predicted with the use of the critical frequency definition by Randall F. Barron but using the model presented by David A. Bies in reference to Davy as seen in Figure 11 section 5.3.4.
4. The Randall F. Barron model proposed for double leaf transmission loss predictions, gives values that are much greater than those by the examined software in the low frequency range. It is recommended to replace the values below the critical frequency with the predictions from the Marshall Long model obtaining a full curve under the normal incidence transmission loss and over the diffuse field transmission loss as seen in Figure 10 in section 5.3.3.
5. The SoundFlow user interface considers different user and how they might organize themselves when working, leading to an easier and more adaptive user interface.
6. Even though the definitions given by the authors B.H.S Sharp and David A. Bies are different for the bending impedance, these share a similar behavior as can be seen in Figure 12 and Figure 16 as well as Figure 13 and Figure 17.
7. The dBKAisla software is useful for transmission loss predictions that are under 80 [dB]. That means that the target value for its transmission loss should be no greater than 80 [dB] to get reliable predictions. On the other hand, SoundFlow is an excellent tool to calculate transmission loss for any structure at target values above 80 [dB] as seen in figure nine section 5.2.3.
8. Looking at Figure 6 in section 5.3.1, the models used from Randall F. Barron, Marshall Long and David A. Bies for the mass law theory have a higher agreement with the SoundFlow normal incidence predictions as opposed to the K.O. Ballagh mass law theory which shows better agreement with dBKAisla.
9. Looking at Table 11 and Table 13, it can be seen, that the variance of cases 7-13 increase as the thickness of the structure increases while in cases 1-6 it remained the same.



## Bibliography

- A. Bies, D., & H. Hansen, C. (2003). *Engineering noise control theory and practice* (third edit). New York: Sponpress.
- Ahnert, A., Media, F., & Ease, C. (2011). AFMG SoundFlow Developed by, (July).
- Ballagh, K. O. (2004). Accuracy of Prediction Methods for Sound Transmission Loss, *47*(1), 1–8.
- Barron, R. F. (2003). *Industrial Noise Control and Acoustics*. New York.  
<http://doi.org/10.1201/9780203910085>
- BSI Standards Publication Acoustics — Field measurement of sound insulation in buildings and of building elements Part 1 : Airborne sound insulation. (2014), (June).
- Cambridge, J. E. (2012). The Sound Insulation of Cavity Walls.
- Kurra, S. (2012). Comparison of the models predicting sound insulation values of multilayered building elements. *Applied Acoustics*, *73*(6–7), 575–589.  
<http://doi.org/10.1016/j.apacoust.2011.11.008>
- Long, M. (n.d.). *Architectural Acoustics*.
- Mak, C. M., & Wang, Z. (2015). Recent advances in building acoustics: An overview of prediction methods and their applications. *Building and Environment*, *91*, 118–126.  
<http://doi.org/10.1016/j.buildenv.2015.03.017>
- SHARP, B. H. S. (1969). The transmission loss of multilayer structures. *Journal of Sound and Vibration*, *9*(3), 383–392. [http://doi.org/10.1016/0022-460X\(69\)90178-3](http://doi.org/10.1016/0022-460X(69)90178-3)